THE DECOMPOSITION ECOLOGY AND MICROBIAL FORENSICS OF THE POSTMORTEM MICROBIOME

A Paper
Submitted to the Graduate Faculty
of the
North Dakota State University
of Agriculture and Applied Science

By

Adam Patrick Ewald

In Partial Fulfillment of the Requirements
for the Degree of
MASTER OF SCIENCE

Major Department:
Microbiological Sciences

July 2021

Fargo, North Dakota

North Dakota State University
Graduate School

Title

The Decomposition Ecology and Microbial Forensics of the Postmortem Microbiome

By

Adam Patrick Ewald

The Supervisory Committee certifies that this disquisition complies with North Dakota State University's regulations and meets the accepted standards for the degree of

MASTER OF SCIENCE

SUPERVISORY COMMITTEE:

Dr. Penelope Gibbs
Chair

Dr. John McEvoy

Dr. Christopher Colbert

Approved:

11/22/2021
Date

Dr. John McEvoy
Department Chair

ABSTRACT

Every living organism dies and is decomposed into nutrients and by-products. This is lead initially by the normal flora of the newly deceased host. The postmortem microbiome, so-called “necrobiome”, undergoes temporal changes affected by the environment in the carcass. The increased data on the necrobiome is fueled by recent advances in genome sequencing analysis techniques. Metagenome sequencing analyzes temporal changes in a population. Genotypic information elucidates identity, structural, and functional traits across a biome. Initially, the necrobiome is composed of taxa common to the living tissue. As decomposition progresses, new and unique taxa emerge. Those suited for growth in the specific environment become dominant. Alpha diversity, beta diversity, and community traits are used to analyze the necrobiome. The necrobiome has potential for forensic evidence predictions. This review covers the succession of the necrobiome specific to body location, their effect on the decomposing carcass, and potential forensics uses of the necrobiome.

ACKNOWLEDGMENTS

I would like to express my gratitude to the chair of my committee, Dr. Penelope Gibbs, who help me through every step of the writing process. I would also like to thank Dr. John McEvoy and Dr. Chris Colbert, who served on my committee, for their help with input into the content of this paper.

TABLE OF CONTENTS

LIST OF TABLES

LIST OF FIGURES

LIST OF ABBREVIATIONS

16S	16 Svedberg
ADD	Accumulated Degree Days
BLAST	Basic Local Alignment Search Tool
CDI	Cadaver Decomposition Island
COD	Cause of Death
MOD	Manner of Death
NCIB	National Center for Biotechnology Information
OTU	Operational Taxonomic Unit
PICRUSt	Phylogenetic Investigation of Communities by Reconstruction of Unobserved States
PM	Postmortem
PMI	Postmortem Interval
RDP	Ribosomal Database Project
rRNA	Ribosomal Ribonucleic Acid
sOTU	Sub- Operational Taxonomic Unit

1. INTRODUCTION TO THE POSTMORTEM MICROBIOME

Every living being eventually dies and thus begins the process of decomposition. Decomposition is led by the postmortem microbiome, also known as the necrobiome. The necrobiome is defined as the eukaryotic and prokaryotic species associated with decomposition of all times including that of human and animal corpses(1). The necrobiome has been shown to have drastic and changes that effect and are affected by their environment. The knowledge base in this field is constantly growing due to advances in the accuracy and affordability of genome sequencing. The environment of a decomposing body is also constantly changing. These changes are predictable and allow the composition of the microbial community to follow a predictable successional pattern. This predictable succession may allow for identification of the postmortem interval (PMI) based solely on the composition of the necrobiome.

This community is initially dominated by resident species. Those taxa that flourish during the shutdown of bodily function and the immune system are integral in the decomposition process. As decomposition progresses, systemic cell death spreads through the body, creating an environment now low in immune response and rich in nutrients that microbes can utilize. The environment of a decaying body is constantly changing though out the decomposition process. These temporal changes affect the structure of the necrobiome allowing the microbes that are best suited to the specific conditions at the time, outcompete less suited microbes. The necrobiome is first noticeable in areas with high resident microbial presence like the mouth, gut and rectum. These will be the first to show signs of decomposition(2). There is a significant lag before organs considered sterile during life such as liver, heart, kidneys, lymph nodes start showing signs of decomposition(2). The resident microbes initiate the process shortly after death and utilize the nutrients left behind from cellular breakdown to multiplying and spread to

previously sterile regions. This is supported by common gut microbes being identified in sterile regions and by a significant increase in motility genes after 48 hours post mortem(3). Infection into sterile regions varies across body site with the liver being positive for bacteria after 1 day postmortem to the pericardial fluid in which 50% of samples were still sterile after 5 days postmortem(4).

Resident microbes that are abundant initially are soon outcompeted by microbes that were previously in low abundance which are now able to flourish in the new environment created as decomposition progresses(5). External communities like the mouth and skin and rectum are directly exposed to the environment which causes more rapid changes(3). The internal communities in areas like the gut are more isolated and influenced more by the biochemical processes involved with internal decomposition such as oxygen depletion and pH changes(3). Understanding the succession of the necrobiome has the potential to aid to the study of decomposition, metagenomics, and forensics alike.

2. CHEMICAL AND PHYSICAL CHANGES OF THE DECOMPOSITION ENVIRONMENT

The environment of a decomposing body changes in a predictable manner which forces the composition of the necrobiome to change along with it. Cobaugh et al 2015 found that there is no change in total microbial abundance in soil communities when a carcass is present but instead, distinct changes in community function and composition(6). They found two distinct changing points in microbial community: when the carcass ruptures (the turning point between the bloat stage changes to the active decay stage), and when the tissue is decomposed and decay rates slow (when active decay stage turns to advanced decay)(6).

2.1. Stages of Decomposition

Decomposition of human remains is a continuous succession of events without distinct stages. In order to aid in discussion, Payne et al 1965 divided decomposition of above ground fetal pig carcasses into 6 stages(7). In chronological order the stages are fresh, bloating, active decay, advanced decay, dry, and remains(7). Dry and remains are very similar from a necrobiome standpoint and are combined for discussion in this paper as “dry remains”(6).

Figure 1. The Stages of Decomposition. Pictured is the carcass of a 10 week old pig. (a) Depicts bloat stage approximately 48 hours PM. (b) Depicts active decay. (c) Depicts active decay. The arrow shows the path of maggot migration, and the bar represents 1 meter. (d) Depicts the dry stage of decomposition(8).

2.1.1. Fresh

The fresh stage begins at death and lasts 24 to 48 hours. This is the most complex stage due to the sheer number of changes that occur internally(7). Immediately after death the heart stops circulating blood and the oxygen present is rapidly consumed, limiting oxygen supply and effectively ending aerobic respiration(8). After the heart stops pumping, the first noticeable changes from a forensics standpoint are called livor, rigor, and algor mortis(9, 10). These stages occur simultaneously and are initiated at death. In the first 1-2 hours, blood migrates by gravity

and pools at the bottom of the carcass in a process called livor mortis(9). This pooling is fully developed by 6 hours and causes a discoloration of the skin(10). After livor mortis, the next visible sign of decomposition is the stiffening of muscles called rigor mortis (9, 10). Rigor mortis is fully developed at 24 hours and by 48 hours, muscles begin to decompose and start to loosen up(9). Algor mortis starts shortly after death and is the slow cooling of a body to ambient temperature(9, 10). Algor mortis proceeds from body temperature to ambient temperature at an approximate rate of 1.5°F an hour. Underlying these processes is cellular death via autolysis.

Autolysis is independent of bacterial action and is caused by hydrolytic enzymes self-digesting proteins and cellular membranes(10). This is the first major destructive process of tissue decomposition(10). Autolysis causes skin slippage which is when the epidermis is loosened from the dermis(9). This can be visualized as early as 48 hours and the hair and nails will become loose and eventually fall off(9). Tissues are mostly free of bacteria for the first 24 hours after death but autolysis releases nutrients that facilitates the initiation of putrefaction across the body(10). Under natural conditions, insects (generally flies of the Sarcophagidae and Calliphoridae families) begin to colonize carcasses at this time lay eggs in soft tissue(7, 8). The color of the skin will slowly change from a red tone to purple as hemoglobin is converted to deoxyhemoglobin in a process called marbling(8, 9). Marbling combined with gas build up caused by bacterial growth are the initial sign that decomposition can now be described as the bloat stage(8).

2.1.2. Bloat

Bloating is caused by the buildup of gasses produced by the bacterial proliferation present in a decomposing body. This stage generally starts at about 48 hours and lasts for 2 days(7). Figure 1a depicts a 10 week of pig in the bloat stage(8). Noticeable signs of this stage

are stiffening of the limbs, marbling, and pressure buildup of gasses, specifically in the abdomen that causes the bloated state of the carcass(8). Hydrolysis of macromolecules is initiated by autolysis, but it is slow until the bacteria take over during the bloat stage(10). The Lactobacillales family Lactobacillaceae is abundant during the initial stages of decomposition but decreased as PMI increased(11). Putrefaction yields gasses including CO_2, methane, hydrogen sulfide, and ammonia are caused by the breakdown of and carbs, alcohols, and organic acids(10). Hydrogen sulfide can react with the porphyrin ring of hemoglobin to form sulfhemoglobin which produces a green color that can be noticed during marbling(10). More flies from the families Piophilidae and arrive and colonize the carcass(7). As pressure builds, bodily fluids are purged from the mouth and nose creating nutrient islands for decomposers(9). Excessive pressure with the help of maggots often times causes the rupture of the abdomen which is the main sign of the start of the active decay stage(9).

2.1.3. Active Decay

Active decay is generally from day 3 to day 6 and is a period of rapid biomass loss(7, 9). Figure 1b depicts a carcass during active decay(8). The most noticeable sign of this stage is the rupture of the skin caused by gas build up due to microbial activity(8). Rupture releases large amounts nutrients into the soil while also, exposing the internal microbial communities to oxygen(9). This shift causes the previously anaerobic internal environment to become rapidly oxygenated significantly changing the microbial communities(12). An example of this community is presented in Figure 2(12). In Figure 2, Lactobacillaceae and Lachnospiraceae are both in high abundance initially in the abdomen but decrease significantly as decomposition progresses(12). Bacteroidaceae increase through active decay then decrease through the end of sampling(12). Xanthomonadaceae, Caulobacteraceae, and Sphingomonadaceae remain at steady

abundance levels initially until late active decay where they increase significantly(12). Anaerobic gut originating genera like *Lactobacillus* and *Bacteroides* are quickly outcompeted by aerobic soil originating Alphaproteobacteria and gut originating *Proteus* and *Escherichia*(12). The genera *Ignatzschineria* is commonly associated with the fly species *Wohlfahrtia magnifica* of the Sarcophagidae family and is introduced through the fly larvae and proliferates in the bloat through active decay stages(13). Fly larvae from Sarcophagidae and Calliphoridae are prevalent initially and Piophilidae and Lonchaeidae begin to proliferate at this stage(7). This maggot activity combined with bacterial communities rapidly consume the remaining tissues(8, 9). As most of the tissue is consumed, the carcass enters advanced decay.

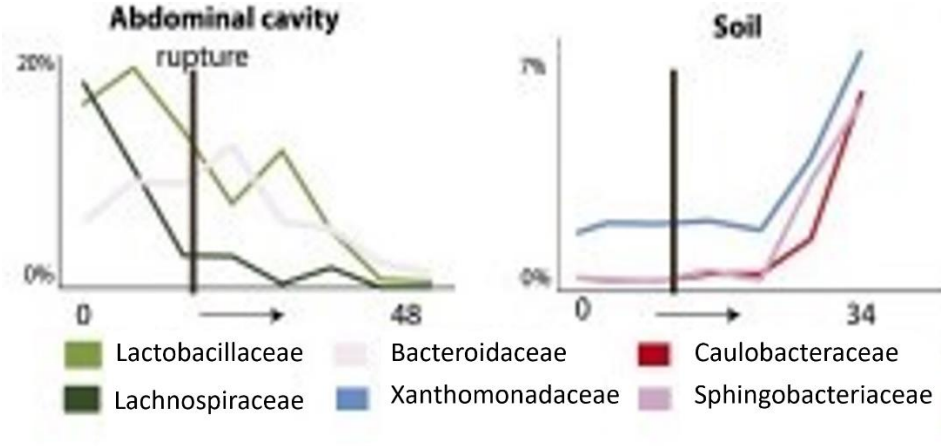

Figure 2. Trajectories of Bacterial Families with the Greatest Change in Abundance. Three families that showed the greatest change in abundance. The black bar represents rupture which occurred between sample day 6 and 9. Y axis is percent change in abundance and x axis is days PM(12).

2.1.4. Advanced Decay

Advanced decay is the stage of decomposition with an increase in skeletonization percentage. This usually lasts from days 6 to 7(7). During advanced and active decay, the soil has a major increase in carbon, nitrogen, and pH(9). Advanced decay is depicted in Figure 1c(8). The release of decomposition fluids and maggot activity form a cadaveric decomposition island

(CDI)(8). A CDI is visible in Figure 1c and Figure 1d(8). Advanced decay proceeds until the body starts to dry and is completely skeletonized.

2.1.5. Dry Remains Stage

Dry remains is the final stage of decomposition and only bone, cartilage, and skin remain(7). The remains are very low in nutrients but the soil is still higher in nutrients than it was previously(9). The flies that colonized the carcass through the early stages of decomposition are replaced by soil originating insects like centipedes and millipedes(7). Figure 1d depicts a cadaver during the dry stage of decomposition(8). This is denoted by the lack of biomass present on the cadaver, the CDI still present due to the increase in nutrients from the cadaveric fluids, and increased plat growth surrounding the CDI(8).

2.1.6. Conclusions

Decomposition proceeds through a predictable succession of events and analysis of these events will aid in understanding necrobiome and how it may aid in identification of the postmortem interval. The postmortem microbiome is becoming a major new subject of study within decomposition due to increasingly affordable prices of whole genome and 16S rRNA sequencing. Cellular death is a major piece in decomposition and proceeds through one of 3 main pathways. These pathways are apoptosis, autophagy, and necrosis.

2.2. Pathways of Cellular Death

2.2.1. Apoptosis

Apoptosis is a regulated pathway of cellular death where the cell blebs and forms apoptotic bodies which are up taken by phagocytes and degraded(14). The process of apoptosis starts with chromatin condensation (pyknosis), followed by nuclear fragmentation (karyorrhexis). Then membrane blebbing creates apoptotic bodies which, under most conditions,

are absorbed and degraded by neighboring cells such as phagocytes(15). Apoptotic bodies are intact vesicles containing contents of the fragmented cell(14-16). Caspases, which commonly accompany apoptosis, are highly conserved cysteine proteases that cause an intracellular caspase-cascade which activates apoptosis(17). Caspases act as both initiator to begin the signaling of apoptosis and as executioner to cleave major substrates in cells(17). Under standard conditions, not involving systemic death, programmed cellular death most often follows the apoptosis pathway(14, 16). Early in decomposition, cell death can follow the apoptosis pathway. Evidence shows that early in decomposition apoptotic genes are actively regulated showing increase in apoptotic transcripts 48 hours after death(18). During decomposition, any apoptotic bodies that remain after the immune system stops are broken down and consumed as nutrients by the necrobiome.

2.2.2. Autophagy

Autophagy is programmed cell death through phagocytotic uptake and subsequent breakdown of cells(15, 16). The steps of autophagy in chronological order are cytoplasmic vacuolization, where the cytoplasm is separated into double membraned vacuoles, phagocytic uptake, fusion with lysosomes, followed by degradation from lysosomal hydrolases(16). Autophagic cell death is not typically caused by organismal death which favors apoptosis and necrosis.

2.2.3. Necrosis

Necrosis is cellular death not associated with apoptosis or phagocytosis that causes spillage of cellular contents to intercellular space(15, 16). This “accidental” cell death is a response to extreme physical, chemical or mechanical stressors(16). This largely unregulated cellular death follows a consistent cascade of events. The first noticeable sign of necrosis is the

swelling of the cell (oncosis) and swelling organelles(16). Next, clustering of organelles takes place near the nucleus and activation of the proteases calpains and cathepsins(16). Finally, the rupture of the plasma membrane and leaking of cellular contents into the intercellular space. Necrosis lacks specific biochemical markers and must be visualized under a microscope(16).

2.2.4. Conclusions

Host death causes cellular death to follow one of these three pathways. Different cellular signals determine the pathway used. Apoptosis is initiated through activation of the caspase cascade responding to stimuli such as DNA damage, and death signaling(14). Autophagy is activated through autophagic vacuolization most often responding to local starvation of nutrients. Necrosis is associated with osmotic stress caused by numerous stimuli such as reactive oxygen species and Ca2+ overloading(16). Besides external stimuli, ATP can be a factor in determining the death pathway followed. Low levels of ATP can favor necrosis and a cell that would normally follow apoptosis can shift to necrosis in absence of ATP(16). Cell death that normally manifests through apoptosis can shift to autophagy or necrosis through prevention of caspase activation(16). Similarly, autophagy can be shifted to apoptosis or necrosis through inhibition of the early steps of autophagy(16). While systemic cellular death is spreading though the body, the environment of the surrounding soil is significantly affected by decomposition.

2.3. Postmortem Soil Chemistry

As with the necrobiome, the postmortem soil chemistry remains largely consistent through the beginning of decomposition. Rupture of the carcass causes a dramatic increase in nutrients, especially nitrogen, into the soil(5, 6). Cobaugh et al 2015 and Metcalf et al 2013 found rupture causes ammonia rich nutrients to enter soil(6, 12). Metcalf et al 2016 found a change in soil chemistry from an average pH of 6.2 to 8.5(5, 6, 12). Unlike previous studies,

Cobaugh et al 2015 did not find a significant increase in pH corresponding to rupture due high variability in pH between their 4 replicate carcasses(6). This caused the pH to be measured at 7.049 ±1.214 so the pH after rupture was significantly different than the initial or control soils(6). There is an increase in total organic carbon and total nitrogen after rupture which remains significant through late advanced decay(6). This influx of nitrogen rich nutrients in the soil caused by rupture forces the microbiome to increase nitrogen cycling and tolerance to the new chemical environment, which is now nitrogen rich with an increased pH(5). Rupture causes soil ammonium levels to increase to a peak 30 days after the carcass was introduced followed by gradually decline(5). Metcalf et al 2016 found there is an increase in the nitrate concentrations and processes that consume nitrate but did not find genetic signs of increased nitrification rates such as an increase in hydroxylamine dehydrogenase(5). This may be caused by the PICRUSt reference database they used lacking genomes from the soil decomposer community(5). There is a significant increase in amino acid degradation and ammonia production which is a likely cause of the increased nitrogen(5).

3. POSTMORTEM MICROBIOME RESEARCH METHODS

3.1. Operational Taxonomic Units

Both metagenome and 16S rRNA sequencing yield large amounts of unique sequences, but this information does not arrive with any taxa identification. The first step to analyzing these community sequencing data is to separate the sequences into operational taxonomic units (OTU). An OTU is a grouping of all sequences that share a certain percent identity, usually 97% identity to have species level specificity (19). This is refined further by removing reads below a certain abundance level, usually 0.005% abundance. These are removed because they are likely "noise" and reduce the precision of data. "Noise" is defined as all sequences that are caused by errors and are not true sequences from the sample and can often negatively affect the resolution of sequencing(20). This includes single nucleotide errors and chimera sequences of two sequences combined together which can stem from both PCR amplification before sequencing and the sequencing itself(20). Sequencing methods such as Illumina have an error rate of 0.01 to 0.1% which can cause both "noise" and chimera sequences(21). This OTU data is labeled using a database such as BLAST, SILVA, RDP, and Greengenes.

Greengenes is a 16S rRNA gene database that can accurately remove chimeric sequences and label bacterial and archaea taxa(22, 23). Ribosomal database project (RDP) is another 16S rRNA tool that uses data from the International Nucleotide Sequence Database Collaboration (INSDC) to label 16S rRNA sequences and detect anomalies like chimera sequences(24). SILVA (from the Latin word for forest, silva) is a database that can read small and large subunit rRNA from bacteria, archaea, and eukaryotes(25). BLAST (Basic local alignment search tool) is a tool to align biological sequences based off the sequence database from the National Center for Biotechnology Information (NCBI) and gives the statical information about the sequence

alignment(26). A phylogenetic tree using these labeled sequences and similar OTUs are combined if they have the same taxonomic name. This data can now be directly analyzed for relative abundance and alpha diversity metrics such as community richness.

3.1.1. Sub Operational Taxonomic Units

Although OTUs are the most common way to label metagenome data, new methods that avoid grouping based off similar identity are available as well. These newer methods utilize sub operational taxonomic units (sOTU) which use statistics and exact sequences to increase the resolution compared to standard OTUs(27). “Noise” is traditionally controlled with clustering into OTUs all sequences with over 97% identity and with algorithms specifically used to identify and remove error reads(28). These sOTU programs do not combine sequences with 97% identity and only rely on complex algorithms which allow for differentiation of closely related taxa by identifying exact sequences with up to 1 nucleotide specificity(27). The process is similar to OTUs except the samples are analyzed independently with an algorithm to remove “noise” before labeling(27). One of these methods use a program Deblur. It uses error profile statistics to analyze sequences individually and any sequence determined to be an error is removed(27). Deblur was utilized by Belk et al 2018 to reanalyze previous data that used OTU labeling(29). Belk et al 2018 found similar trends to the previous studies but they were able to more accurately predict the postmortem interval(PMI) (1.7 days compared to 2.5 days)(29). After the sequencing data is labeled with taxa, it is ready to be analyzed. These labeled data can now be analyzed by community and taxon specific methods.

3.2. Relative Abundance

The most common tests used to monitor postmortem microbiome are relative abundance, alpha diversity, beta diversity, and machine learning algorithms.(29) Relative abundance is a

simple calculation of the abundance of each taxon compared to the total number of individual reads present in the sample altogether. It is a comparative analysis of abundance and is most used to show trends of specific taxa and the members of a community across many sample sites and time points. Lutz et al 2020 used the differential relative abundances of bacterial classes to compare the postmortem bacterial community structure based on their anatomic location(30). Alpha and beta diversity are used to identify general trends of the community composition across sample sites and time points. Figure 3 shows the change in abundance of taxa associated with the human mouth across the first 12 days of decomposition(31). The significant abundance change presented in the relative abundance chart of Figure 3 is useful to show the direct and significant change in community composition.

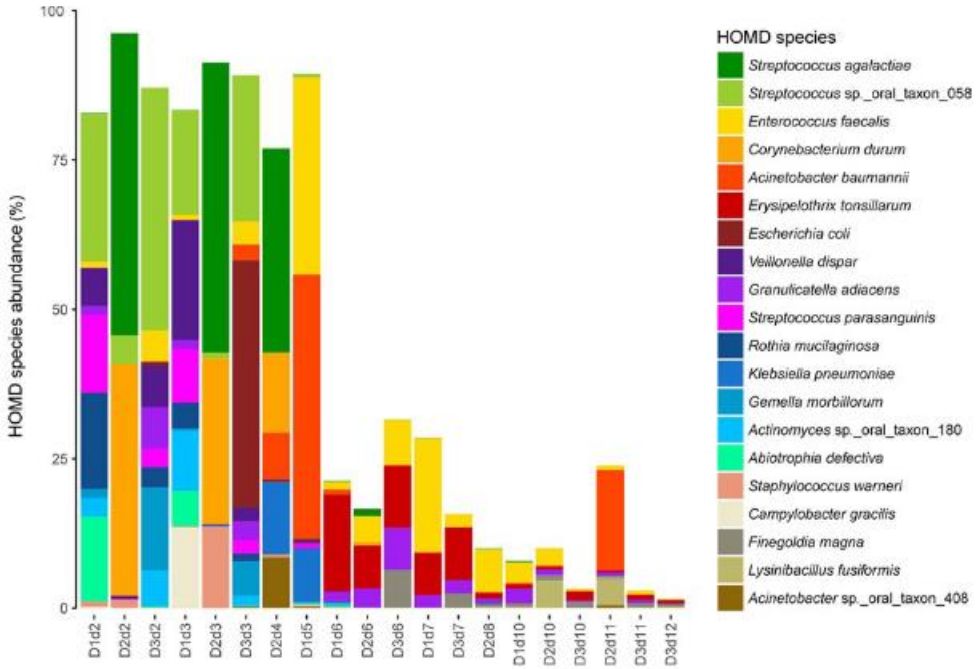

Figure 3. Abundance of Necrobiome Species Found in HOMD. The Human Oral Microbiome Database (HOMD). X axis labeling: “D” is identification number of the corpse 1-3, “d” is days PM(31).

3.3. Alpha Diversity

Alpha diversity is the measure of diversity within a community using richness, evenness or a combination of richness and evenness(32). Richness is the number of different taxa present in a sample which is commonly calculated using the total number of OTU's in a community. Another measure of richness is Faith's Phylogenetic Distance which is shown in Figure 4(3). This calculates richness using the sum of the branch lengths from a phylogenetic tree which includes all species in a population(33). Evenness is a measure of the distribution of abundances of the OTU's within a community. These are used to analyze a community and determine the diversity within each community. This can show if conditions allow a diverse community with a large number of low abundance taxa or if the conditions select for a small number of specific taxa in high abundance. Figure 4 shows the alpha diversity of postmortem bacterial communities from several anatomic locations and that there was a significant decrease in the in richness after 48 hours postmortem(3). This shows that as decomposition progressed, the were lower numbers of unique taxa and the community was made up of specific taxa suited to the conditions(3). DeBruyn et al used a calculation that accounted for both richness and evenness called Sipson's Index(34). This showed that even though the richness of their postmortem gut communities increased after rupture, the Simpson's Index decreased(34). This shows the different forms of alpha diversity measurements can have different results. Alpha diversity metrics are highly biased by read number. Read number can be controlled with rarefaction which is randomly trimming all samples to the same number of reads, or to the lowest number of reads(32). Removing reads using rarefaction can cause its own biases in alpha diversity measures but lowering the observed alpha diversity(32). Errors like these require researchers to use multiple

different measures of diversity to understand an ecosystem. Another diversity metric, beta diversity analyses differences between samples to determine the diversity between samples.

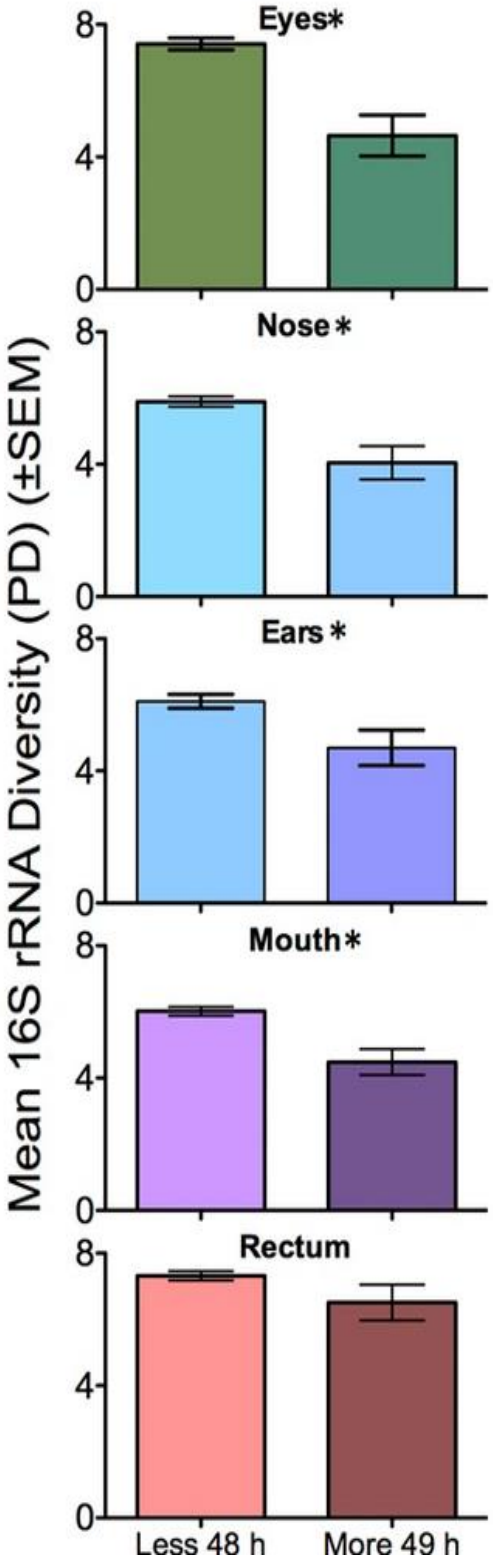

Figure 4. Faith's Phylogenetic Distance of Necrobiome Before and After 48 Hours. Separated by anatomical location(3).

3.4. Beta Diversity

On the other hand, beta diversity measures the diversity between communities or samples. It measures how similar or dissimilar the samples are to each other. It is commonly presented with a distance metric such as UniFrac distances or Bray-Curtis distance are visualized with principal coordinate analysis (PCoA) plots. PCoA plots visualize the beta diversity as distances between points. The more distant the points are apart, the more diverse they are. These plots are commonly used in postmortem microbiome studies to compare different sample locations, different sample times, and compare repeated samples. Figure 5 shows the PCoA of the necrobiome grouped by anatomical location(3). Figure 5 shows distinct grouping by anatomical location, especially noticeable with the rectum which had a grouping with minimal overlap with samples from other locations(3). Bray-Curtis dissimilarity is a measure of differences between communities using taxon abundance differences in each community(35). This is a taxon-based measure and does not account for relatedness of taxa present, it only accounts for the abundances of taxa in each community(2, 35). This method relies on abundance changes with no phylogenetic assumptions and is useful for communities with a high number of unclassified taxa. Burcham et al 2019 used Bay-Curtis dissimilarities of postmortem bacterial communities to find significant diversity differences across both anatomical location and time since death(2).

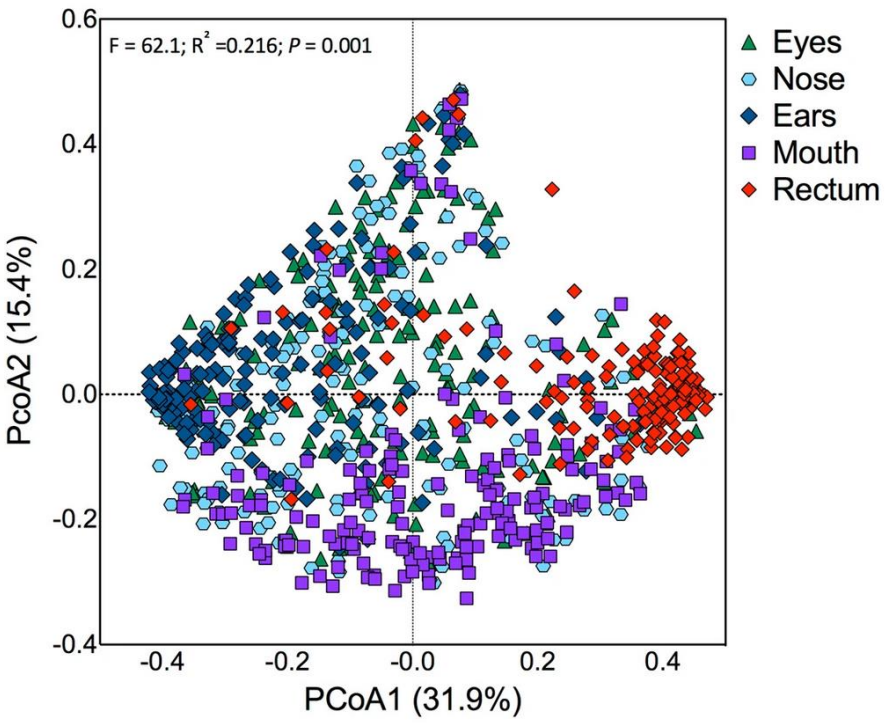

Figure 5. Principal Coordinate Analysis (PCoA) of Necrobiome. Necrobiome beta diversity based on anatomical location(3).

3.4.1. Distance Matrices of Beta Diversity

UniFrac measures the phylogenetic difference between the sequences of 2 samples, generally 16SrRNA in postmortem microbiome studies(36). This is a measure of the evolutionary distance of all sequences in one sample(36). UniFrac can be either weighted or unweighted. Weighted is a quantitative measure that accounts for relative abundance, and unweighted is a qualitative measure that does not account for abundance(36). These different UniFrac measures can lead to dramatically different conclusions with the same samples. Unweighted UniFrac distance is well suited for detecting the presence or absence of specific bacteria in different communities(37). Weighted UniFrac distance is well suited for detecting differences in abundance even when the taxa present remain the same(37). Damann et al 2015 used weighted UniFrac distances to visualize differences in bacterial community members and used weighted UniFrac distances to measure different taxon abundance to visualize changes in

community structure(38). They found differences in beta diversity between bacterial communities sampled from the same bones at different stages of decomposition with unweighted UniFrac distance but not weighted(38). Guo et al 2016 compared the weighted and unweighted UniFrac distances of mouth and rectum necrobiome bacterial communities and found the weighted UniFrac distances had more notable clustering of the two communities as decomposition progressed(39). Kaszubinski et al 2020 compared weighted and unweighted UniFrac distances and found unweighted UniFrac distances had three times the number of significant comparisons between postmortem bacterial communities and manner/cause of death(40). They used beta diversity of postmortem bacterial communities to make predictions on the cause of death of the individual(40). The combination of analyses using relative abundance, alpha diversity, and beta diversity necessary for researchers to sufficiently analyze the composition and diversity of microbiome communities. Complex forms of analysis such as machine learning can aid in classifying necrobiome samples in specific groups.

3.5. Machine Learning Analyses

Machine learning models are analyses techniques that, for microbiome studies, are used to classify large datasets of taxa accurately into groups. The specifics of how these algorithms work is beyond the scope of this paper, but Random Forest regression and k-Nearest Neighbor regression are the machine learning methods most common with the postmortem microbiome and will be mentioned in this paper. Figure 6 presents the mean error from machine learning analyses predicting postmortem interval (PMI)(12). Figure 6 shows Random Forest models of the postmortem microbiome of the skin on the head of mice was most accurate in estimating PMI with an accuracy of 3.30+/- 2.52 days(12). Metcalf et al 2013 found the populations during early decomposition were most accurate when they sampled it the most frequently(12). Johnson et al

2016 tested the PMI prediction accuracy of numerous machine learning methods to see what was most accurate with their ear and nose postmortem microbiome dataset(41). They found k-nearest neighbor regression to be the most accurate with predictions of up to 55 accumulated degree days accuracy for PMI prediction(41).

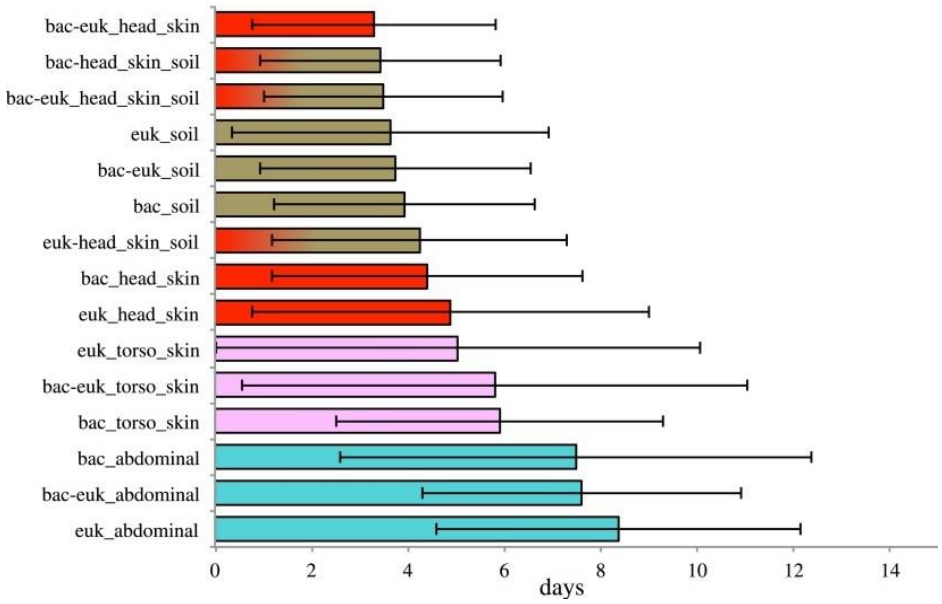

Figure 6. Mean Error of PMI Prediction. Machine Learning analysis used to predict postmortem interval(12).

4. SUCCESSION OF THE NECROBIOME

4.1. Gut and Rectum Necrobiome

The gastrointestinal tract harbors the most diverse microbiome in the human body. This diverse microbiome is able to flourish during decomposition as the cells lyse and the immune system begins to break down. In the gut, normal flora taxa from Bacteroidetes and Firmicutes dominate the nutrient rich environment of the fresh stage of decomposition. More specifically, the Eubacteriales (Lachnospiraceae and Oscillospiraceae) Bacteroidales (Parabacteroideaceae, Bacteroidaceae, and Prevotellaceae), and Lactobacillaceae. Using qPCR in human carcasses, the families Lactobacillaceae and Bacteroides dominate initially in decomposition but their relative abundances decrease over time as they are outcompeted by bacteria better suited to the changing environment of the decomposing carcass(11). Another study supported this trend in the large intestine with the Lachnospiraceae, Lactobacillaceae, and Bacteroidaceae(34). These families dominate during the fresh and bloat stage but become insignificant during active and advanced stages(34). The initial postmortem microbiome is dominated by Firmicutes and Bacteroidetes but as bloat advances towards active decay, Proteobacteria become abundant. The necrobiome of the fresh and bloat stages are presented in Figure 7.

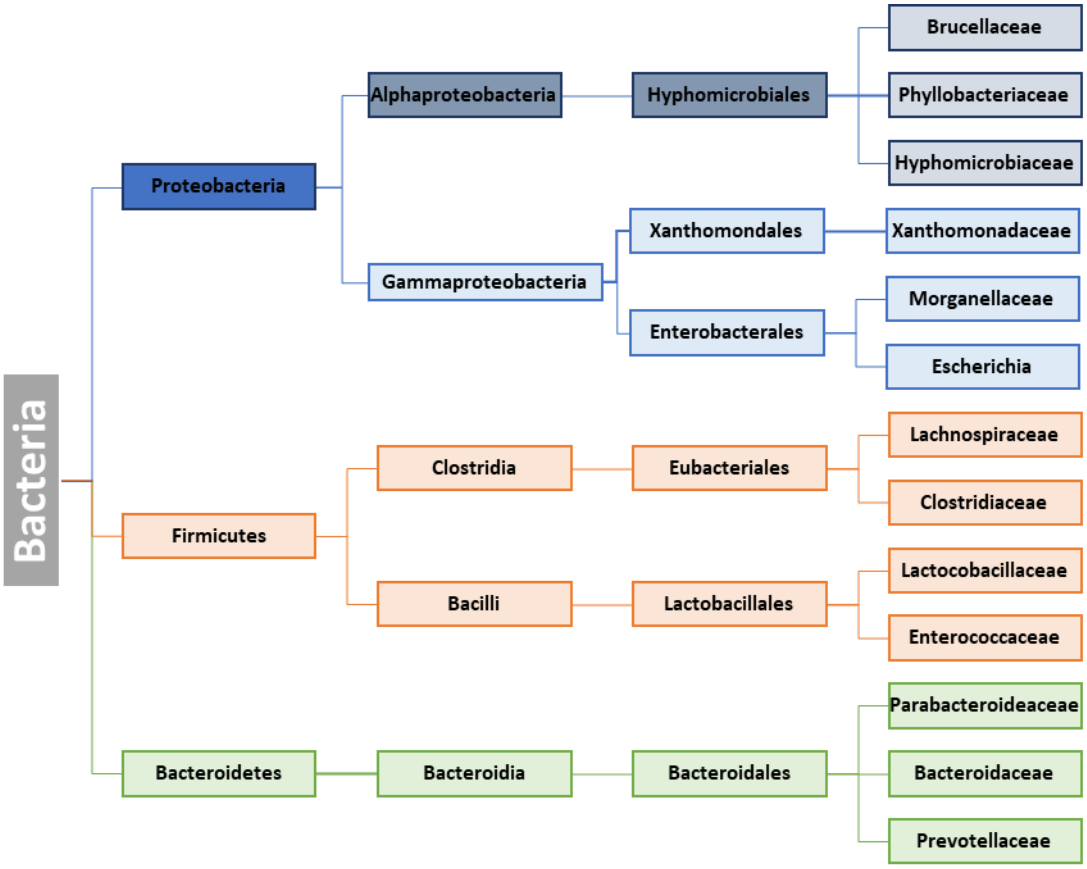

Figure 7. Postmortem Gut Microbiome Taxa Prominent During Decomposition. Only taxa with an abundance of over 5% were included. National Center for Biotechnology Information(NCIB) database was used for all phylogenetic trees using the taxonomy browser tool(42).

During the fresh and bloat stages the families Lachnospiraceae, Oscillospiraceae and Lactobacillaceae, and Bacteroidetes, specifically Bacteroidales, dominate(12, 39). Enterobacteriales families Enterobacteriaceae and Morganellaceae begin rising in abundance during the bloat stage, commonly on the last sample before rupture(12, 39). This trend continues through advanced decay(39). *Proteus* becomes the predominant taxon at abundances of over 80% of the total bacterial community after being in very low abundance early in decomposition(39). This is visualized in Figure 8(39). Also shown in Figure 8, Xanthomonadaceae become abundant in advanced decay which was not present in the fresh stage and in very low amounts during the bloat stage(39). The genus *Ignatzschineria*, of the

family Xanthomonadaceae, increases with PMI and is associated with an insect that are found on decomposing carcasses, *Wohlfahrtia,* also known as flesh flies(43).

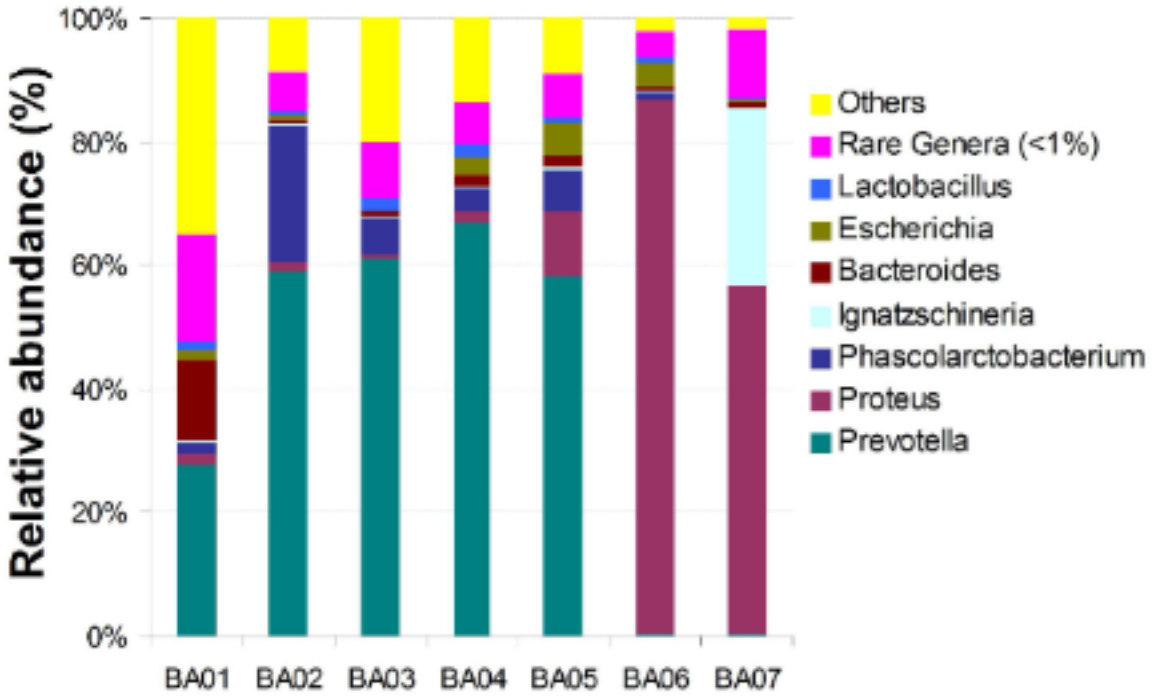

Figure 8. Relative Abundance of the Rectum. Necrobiome of rats from sample times across decomposition. X axis decomposition times are as follows: BA01 – alive, BA02 – 0 hours PM, BA03 – 4 hours PM, BA04 – 12 hours PM, BA05 – 1 day PM, BA06 – 2 days PM, BA07 - 3 days PM. Rupture occurred at day 2 PM(39).

As decomposition progresses, the same phyla, and many of the same orders, remain abundant. Firmicutes is dominant during fresh and bloat and remains abundant through advanced decay, with different families abundant. The Eubacteriales families Lachnospiraceae and Oscillospiraceae are abundant early in decomposition but Clostridiaceae is abundant during active and advanced decay(2, 34). Clostridiaceae has the greatest increase in abundance in all taxa in the gut necrobiome of mice models(12). *Clostridium* is motile and well suited to thrive in the anaerobic environment of advanced decay and are able to colonize organs presumed to be sterile during life(2). Enterococcus, also from Lactobacillales, became abundant in active and

advanced decay(2, 12). The gut necrobiome from active and advanced decay are also presented in Figure 7.

Enterobacteriales are abundant after rupture and Bacteroidetes and Lactobacillaceae are no longer abundant. The Firmicutes order Eubacteriales stays abundant through decomposition but just with different families. Lachnospiraceae and Oscillospiraceae are abundant early but as decomposition progresses, Clostridiaceae predominant in advanced decay. Xanthomonadaceae, commonly associated with the decomposition fly family Sarcophagidae, is introduced by larvae during fresh and bloat stages and becomes abundant after rupture.

Decomposition has varying effect of diversity of the gut communities. The initial postmortem gut microbiome has lower richness than the soil community for every stage of decomposition(6). Richness increases over time but due to a decrease in evenness, the alpha diversity, calculated with a Simpson's Index, decreases as PMI increases(34). Beta diversity has a significant shift corresponding to rupture that causes a significant increase in variability in communities using Bray-Curtis Similarity(34). This conflicts other studies that used rectal sampling and UniFrac distances instead of intestinal sampling and Bray-Curtis similarity which may show different community profiles between these locations or analyses. Guo et al 2016 found a significant decrease richness and in beta diversity in rectum samples as PMI increased(39). This is supported by a significant decrease in beta diversity in rectum sampling as decomposition progressed in another study(44). Pechal et al 2018 found that there is increased community stability in the first 48 hours after death and there was an increase in variability in samples after 49 hours(3). This is presented in Figure 4(3). The diversity of the postmortem gut microbiome has varying changes across these studies as decomposition progressed, masking any

possible trends for the diversity of the gut necrobiome. The next piece of the necrobiome that will be discussed is the oral necrobiome.

4.2. Oral Necrobiome

The oral microbiome is the second most diverse microbiome in the human body; only the gut is more diverse. Due to the ease of sampling, it is one of the best understood of the living human microbiomes. For this same reason, knowledge of the oral necrobiome is significantly increasing. The mouth is home to a diverse community of largely unculturable species that were unidentifiable until next gen sequencing became available(45). The mouth has two very different major surfaces, the hard surface of the teeth and soft tissue of the cheeks, gums, and tongue which are each home to distinct microbial communities(45). The environment present in a living person's mouth is moist with an average temperature of 37°C and an average saliva pH of 6.7-7. This creates a stable environment for the oral microbiome of the host to thrive(46). After death saliva stops being produced and combined with the direct exposure to microbial communities of the soil and skin, the postmortem microbiome community changes rapidly.

The oral necrobiome is a mixing point between microbes migrating up from the gut and in from the soil and skin which gives it many unique traits. The mouth shares common microbes with all other areas sampled and had an increased richness compared to other locations(47). In a large 2018 study with samples from 188 autopsy cases the mouth necrobiome is the most variable community and the community structure in the rectum necrobiome is the most consistent(3). The PCoA based on unweighted UniFrac distances shows a distinct group for the mouth(47). This means that the mouth had a subgroup within the community with low beta diversity which was significantly different than other sample locations(47). Adserias et al 2016

found in the mouth a unique phylum, Tenericutes, quickly spike in abundance then drop back to unreadable levels in a short time frame corresponding to the bloat stage(31).

Guo et al 2016 found a significant difference in the oral microbes of a living mouse and the microbiome of mice immediately after death(39). These communities have a large amount of overlapping taxa between the living microbiome and the 0 hour postmortem sample but the alpha diversity rapidly increases in the 0 hours postmortem sample compared to the living microbiome(39). This means there are a higher total number of species present. Possible explanations are the immediate halt of saliva production, and the fact the mouth is in close proximity to soil and skin microbes which may be able to migrate easily or contaminate the sample. Another study found the mouth had the lowest prevalence of motility pathways in samples <48 hours(3). This makes motile taxa transmigration into the mouth an unlikely cause for the increase in richness. Saliva has antimicrobial properties so no production of it may cause these new migrating or contaminating species or allow low abundance species to thrive. Other studies did not find a change in the living vs 0 h postmortem samples because they tested either an initial postmortem sample or living mouse, not both.

The initial oral postmortem microbiome is made up of the common living oral microbiome (31, 39, 47, 48). Oral originating taxa are dominant in initial postmortem communities, but this trend changes quickly, and the dominant taxa are soon more often associated with the gut or soil instead of the mouth(31). Figure 3 shows the significant decline in the abundance of species associated with the living human mouth as decomposition progresses into bloat and active decay(31). The prevalence of HOMD associated taxa decreased substantially in their samples from 6-12 days postmortem showing the community was dominated by non-orally originating taxa(31). Proteobacteria and Firmicutes were the dominant

oral phyla initially and through the first days of decomposition with lower but significant levels of Actinobacteria and variable levels of Bacteroidetes(31, 39, 48). To aid in discussion of the oral necrobiome, the families associated with the necrobiomes of the fresh, bloat and active decay stages are presented in Figure 9, Figure 12, and Figure 13.

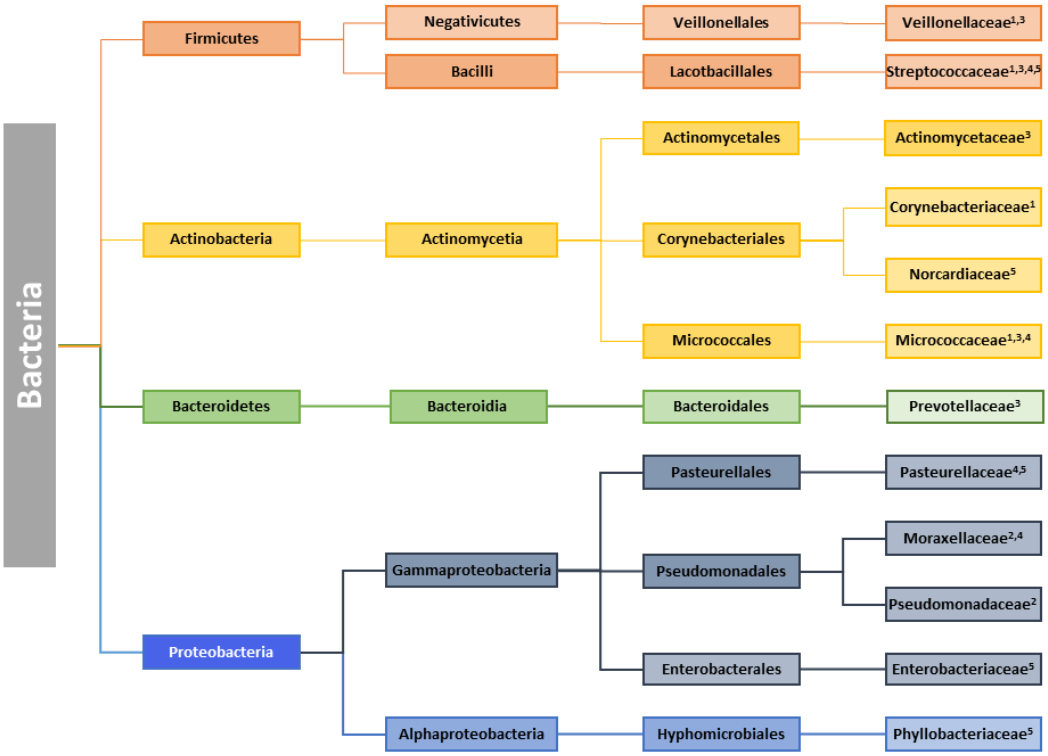

Figure 9. Postmortem Oral Microbiome Taxa Prominent During the Fresh Stage. Only taxa with an abundance of over 5% were included. National Center for Biotechnology Information(NCIB) database was used for all phylogenetic trees using the taxonomy browser tool(42).

The rat and mouse models that Guo et al 2016 and Dong et al 2019, respectively, used as model organisms were dominated by Streptococcaceae and Pasteurellaceae with low amounts of different Actinobacteria families(39, 48). The fresh postmortem microbiome animal model studies each had their own unique families. The mouse necrobiomes have a significant initial amount of the Alphaproteobacteria family Phyllobacteriaceae and an increase in Gammaproteobacteria family Enterobacteriaceae at the end of the fresh stage(48). This is shown

in Figure 10(48). The rat necrobiomes have a significant increase of the Gammaproteobacteria family Moraxellaceae at the end of the fresh stage(31). This is shown in Figure 11(31). Javan et al 2016 studied humans with data collected during autopsies(47). They found the mouth necrobiome is dominated by the families Streptococcaceae Prevotellaceae and Veillonellaceae with notable abundances of unique families Micrococcaceae and Actinomycetes and Staphylococcaceae(47). Hyde et al 2015 used human subjects on natural soil postmortem and differed from the other studies in their fresh samples and did not have significant abundances of anything other than two Pseudomonadales families, Moraxellaceae and Pseudomonadaceae(44).

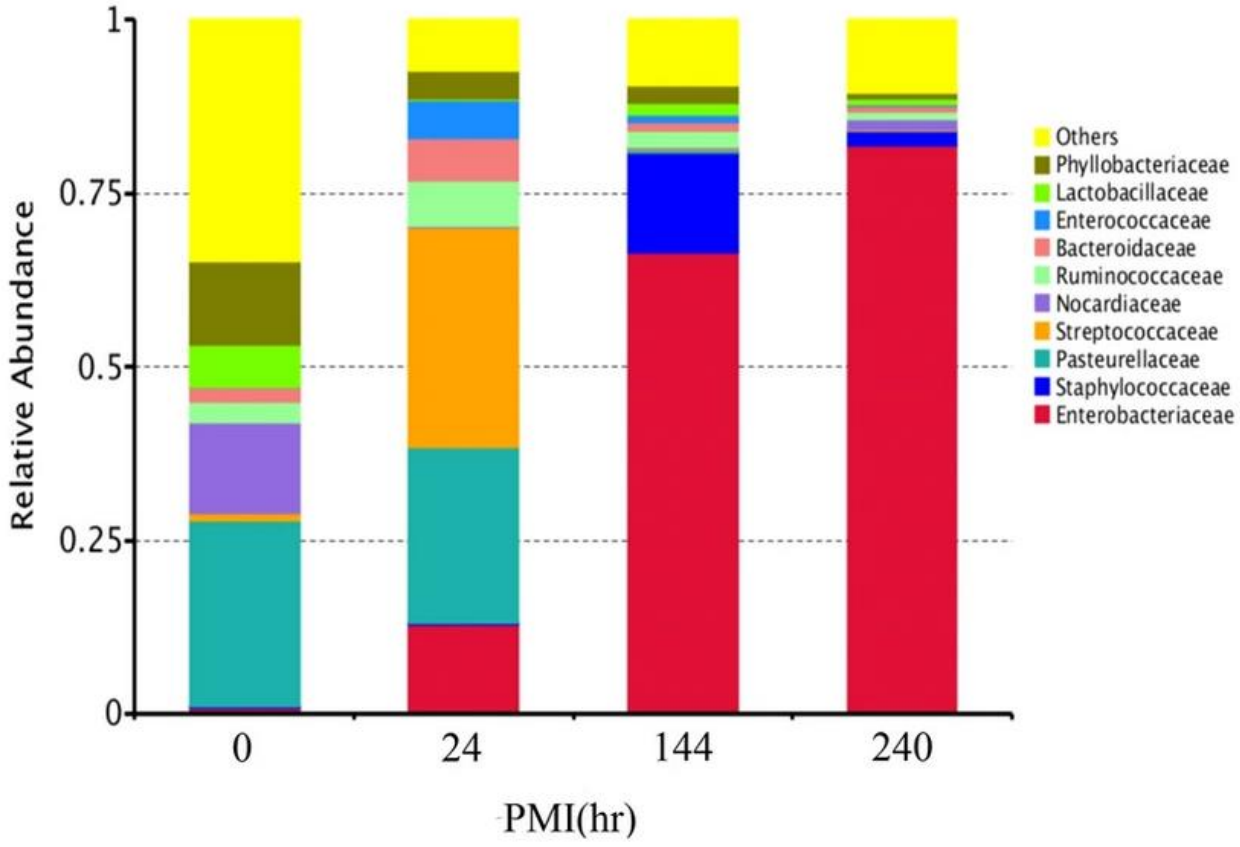

Figure 10. Relative Abundance of the Necrobiome from the Oral Cavity of Mice. Rupture occurred between 24 hours and 144 hours(48).

In the bloat stage, Xanthomonadaceae and Moraxellaceae families increase across the studies and Enterobacteriaceae increase in two of them(31, 39, 44). Two human studies both

have Xanthomonadaceae increase in abundance along with gut associated taxa. Hyde et al 2015 has Moraxellaceae while Adserias et al 2016 has Enterococcaceae as their next most abundant after Xanthomonadaceae(31, 44). Guo et al was dominated by Moraxellaceae in the bloat stage with significant abundances of Enterobacteriaceae, Xanthomonadaceae, and a family unique to them, Flavobacteriaceae(39). This is shown in Figure 11(31). Xanthomonadaceae is associated with insects, but it was found in both the insect and insect free samples which may show it is associated with decomposition without insects as well(31).

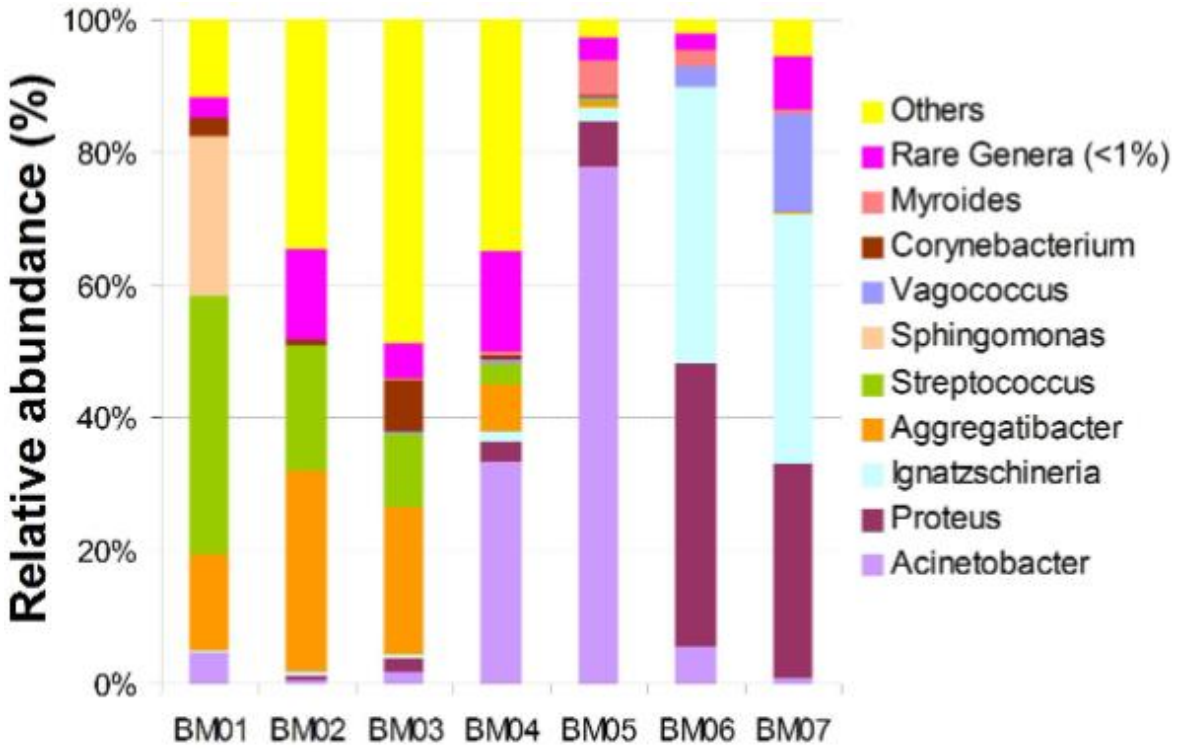

Figure 11. Relative Abundance of the Oral Cavity of Rats. X axis decomposition times are as follows: BA01 – alive, BA02 – 0 hours PM, BA03 – 4 hours PM, BA04 – 12 hours PM, BA05 – 1 day PM, BA06 – 2 days PM, BA07 - 3 days PM. Rupture occurred at day 2 PM(39).

The bloat stage samples are dominated by Gammaproteobacteria, specifically, Moraxellaceae and Xanthomonadaceae, and a rising abundance of Clostridia. This shows a general trend away from the oral associated taxa towards more gut and soil associated taxa. This dramatic shift corresponded to the beginning of the active decay stage. Aerobic normal flora

dominated initially but fermentative Proteobacteria and Firmicutes dominated as the oxygen was consumed(31). The oral microbes are outcompeted by taxa that are uniquely suited the specific environment. These important factors include varying temporal changes in oxygen level, pH, and nutrient availability in each stage of decomposition.

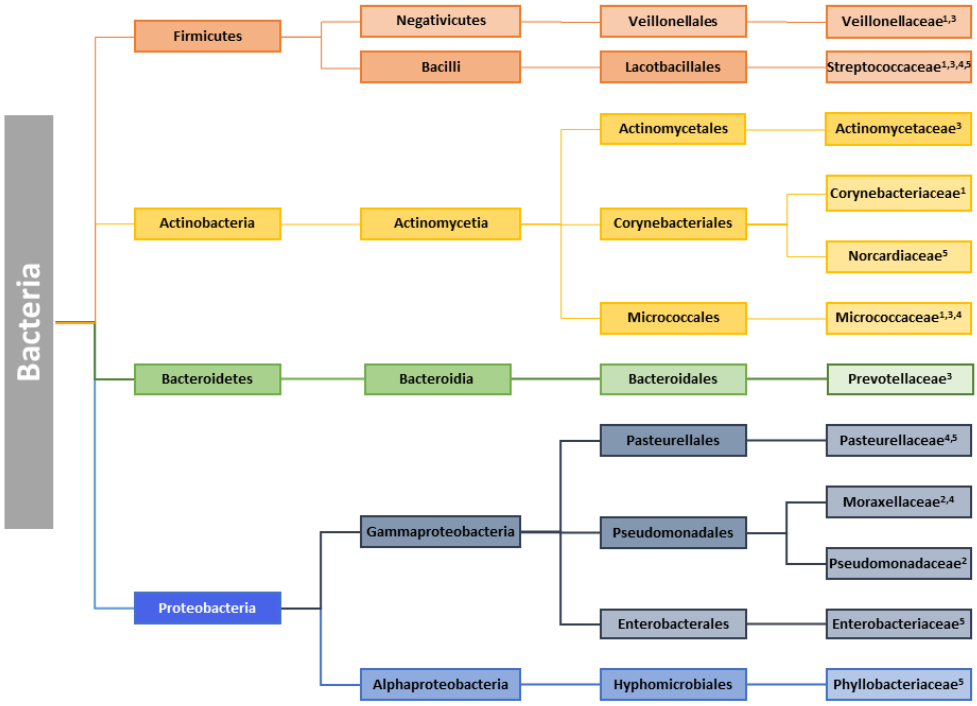

Figure 12. Postmortem Oral Microbiome Taxa Prominent During the Bloat Stage. Only taxa with an abundance of over 5% were included. National Center for Biotechnology Information(NCIB) database was used for all phylogenetic trees using the taxonomy browser tool(42).

In the human studies there is a significant decrease in Xanthomonadaceae from bloat to active decay(31, 44). Active decay has a significant initial abundance in Xanthomonadaceae which is replaced by soil and gut associated families like Corynebacteriaceae, Moraxellaceae and Clostridiaceae(31, 39, 44). Xanthomonadaceae is aerobic and associated with fly larvae commonly found on decomposing corpses(13). A decrease in maggot associated bacteria is correlated with a similar decrease in the total number of maggots present(8). As a cadaver moves through advanced decay and into active decay, the biomass is consumed and the number of

maggots decreases(7, 8). Animal models have a significant increase in Enterobacteriaceae during advanced decay(39, 48). This is associated with the gut and in a study excluding insects, it increased to over 75% abundance in advanced decay(48).

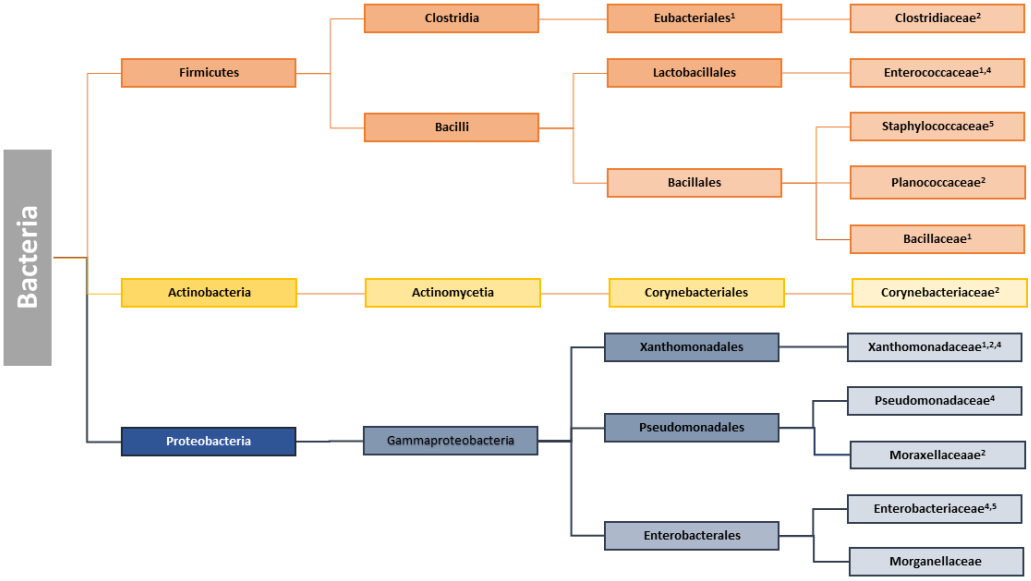

Figure 13. Postmortem Oral Microbiome Taxa Prominent During the Active. Only taxa with an abundance of over 5% were included. National Center for Biotechnology Information(NCIB) database was used for all phylogenetic trees using the taxonomy browser tool(42).

The carcasses are more similar within each experiment at different postmortem intervals than they were within postmortem intervals across experiments(31, 39, 44, 48). These experiments had differing decomposition conditions from more natural decomposition of humans in natural soil to mice in a controlled lab experiment with no soil or insects present(31, 39, 44, 48). The differing soil communities or lack of soil like in laboratory settings on sterile gauze and from the morgue could have a significant difference in the necrobiome(31). These would affect the decomposing carcass in different ways

The initial postmortem oral microbiome varied significantly between studies but was dominated by resident taxa such as *Prevotella, Veillonella, Rothia, Streptococcus, Muribacter*

and *Pasteurella*(31, 39, 44, 48). This change rapidly and by advanced decay, it was dominated by soil, gut, and fly originating taxa such as the Proteobacteria *Proteus, Xanthomonadaceae, Ignatzschineria* and *Enterobacteriaceae* and the Firmicutes Clostridiales, *Enterococcus,* and *Bacillaceae*(31, 39, 44, 48). All studies were dominated initially by Proteobacteria, Firmicutes, Actinobacteria, and Bacteroidetes, but the animal models had a general trend of being increasingly dominated by Proteobacteria and the human trials were dominated by Firmicutes. The soil necrobiome is important for studies that use natural soil conditions and will be discussed next. The skin necrobiome is in direct contact with the soil necrobiome which causes these communities to change in a similar manner.

4.3. Soil Necrobiome

The postmortem soil environment remains largely unchanged from the initial placement of a carcass through the first two stages of decomposition. The steady environment led to a soil necrobiome that remains largely unchanged through the fresh and bloat decomposition stages(6, 12). As the carcass advances from the bloat stage into the active decay stage, pressure builds up and decomposition fluids seep from the orifices until the pressure is too great and the carcass ruptures. This causes a significant increase in decomposition fluids from the chest cavity and the necrobiome along with it(12). The influx of decomposition taxa changes the postmortem soil community to a mixture of soil and decomposition bacteria after rupture. This change causes human associated taxa take over during advanced decay(12). This starts to slowly change in the late advanced decay stage when the nutrients from the decomposition fluids start to run out and soil microbes start to dominate again(6). As decomposition progresses further to dry remains, soil originating taxa like Alphaproteobacteria Acidobacteria, and Actinobacteria become

prevalent again in the postmortem community(6). This is due to the nutrients being depleted and human associated species are outcompeted.

The major phyla of the early postmortem soil microbiome are Proteobacteria, predominantly Alphaproteobacteria, Acidobacteria, with lower levels of Firmicutes, Bacteroidetes, Verrucomicrobia, Actinobacteria, Planctomycetes, and the Proteobacteria class and Gammaproteobacteria and Betaproteobacteria(6, 12). The postmortem initial, fresh, and carcass free control soil microbiomes are combined in Figure 14. These taxa are similar to soil samples from soils without a carcass present(49). An example of taxa associated with soils is shown in Figure 15(38). This shows the soil under a carcass will remain dominated by soil bacteria during the early stages of decomposition(6, 12).

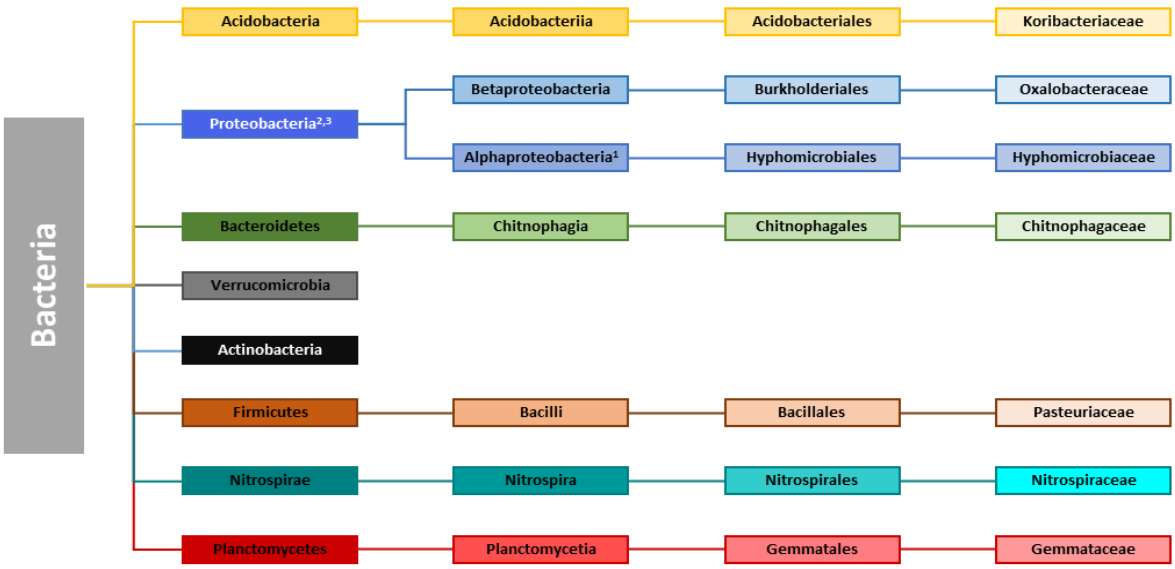

Figure 14. The Initial Postmortem Soil Microbiome. The soil microbiome from the fresh, bloat and controls soils. Only taxa with an abundance of over 5% were included. Phylogenetic tree was created using the NCIB taxonomy browser tool with the exception of Koribacteriaceae(42). Koribacteriaceae was not present in the NCIB database but is a member of the Acidobacteriales order(49).

Rupture causes a significant and lasting change in the soil postmortem microbiome. These changes included a decrease in Acidobacteria and Verrucomicrobia and an increase in Firmicutes and Actinobacteria(12). Lauber et al 2009 found Acidobacteria to be negatively associated with increasing soil pH so as the postmortem soil pH rises after rupture, this supports the decrease in Acidobacteria(6, 12, 50). Acidobacteria are also found to be slower at cellular division and metabolism so increase in nutrient abundance and in pH likely lead to the phyla being outcompeted(51). The invasion of the soil by the gut postmortem microbiome is more notable during the advanced decay stage. Advanced decay had significant decrease in Acidobacteria, Verrucomicrobia, and an increase in Firmicutes, Actinobacteria, and alphaproteobacteria(12). Bacteroidetes, a human associated phylum, increased significantly and persisted in soils up to 198 days, through the end of experimentation(6). Taxa associated with advanced decay are presented in Figure 16. The taxa associated with partially skeletonized and skeletonized remains during advanced decay are shown in Figure 15(38).

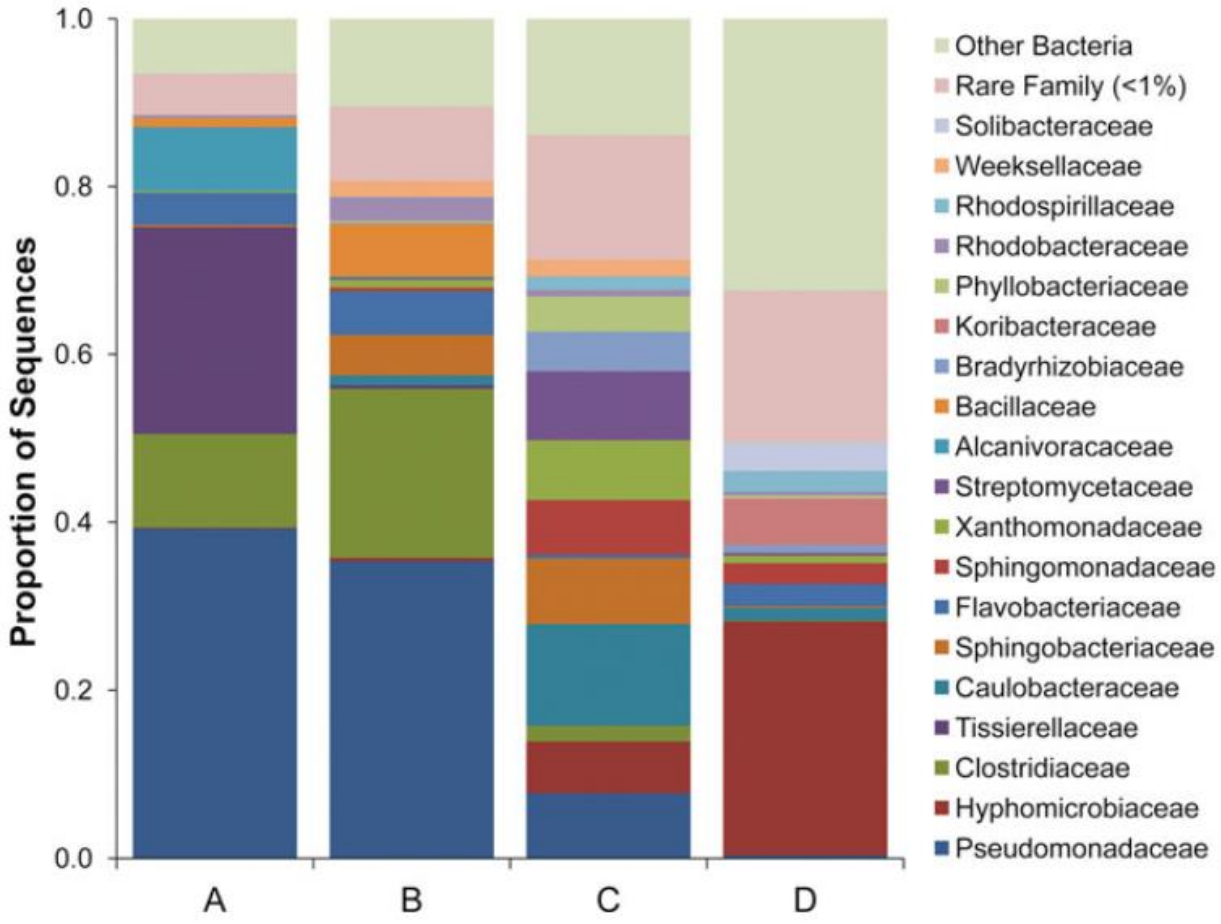

Figure 15. Relative Abundance of the Necrobiome Found on Soil and Decaying Bone. X axis labels are as follows: A – partially skeletonized, B – skeletonized, C – dry remains, D – soil(38).

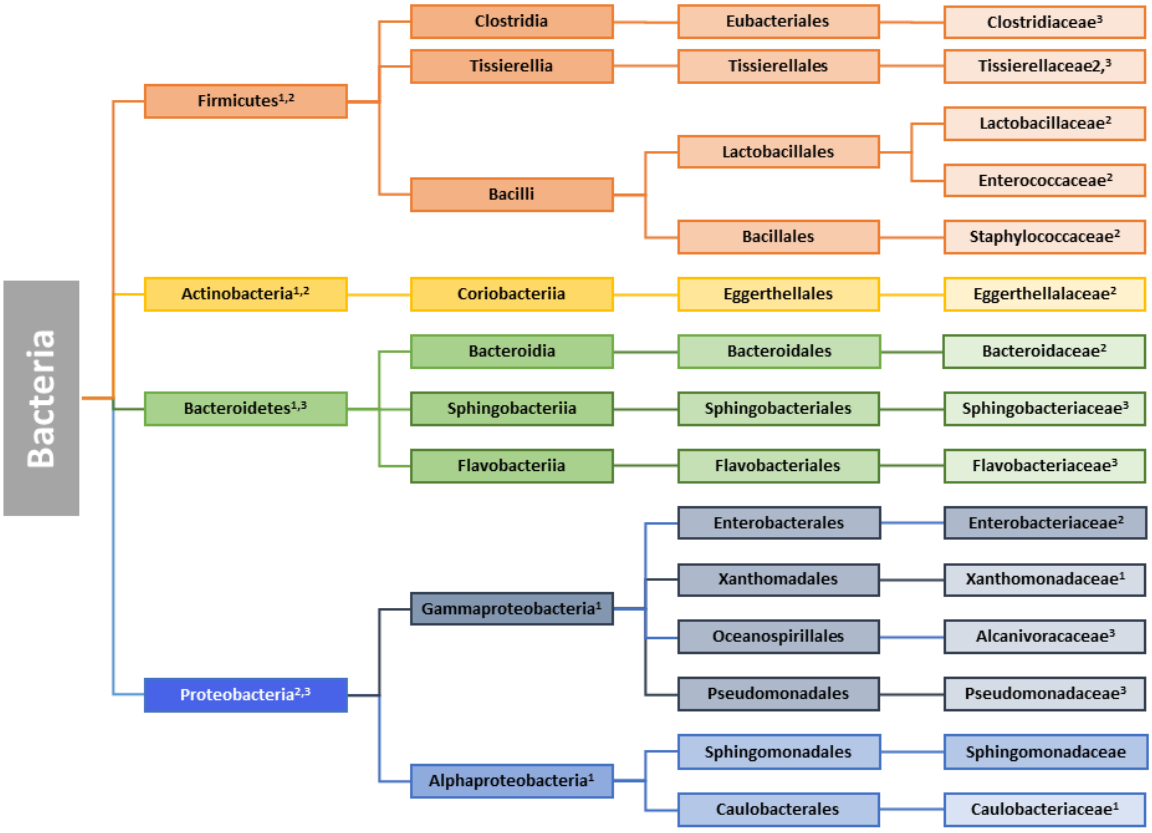

Figure 16. Postmortem Soil Microbiome Taxa Prominent During Advanced Decay. Only taxa with an abundance of over 5% were included. National Center for Biotechnology Information(NCIB) database was used for all phylogenetic trees using the taxonomy browser tool(42).

As decomposition progresses out of advanced decay into the skeletonized and dry remains stages, the necrobiome begins to shift back to soil originating taxa(38). This leads to a significant decrease in Gammaproteobacteria and Bacteroidetes along with an increase in Alphaproteobacteria, Actinobacteria and Acidobacteria(38). Many of these changes were not all visible on the phyla level. For example, Cobaugh et al found Proteobacteria as a phyla remain fairly consistent and abundant in the soils throughout decomposition(6). The taxa present changed with Alphaproteobacteria and Gammaproteobacteria increasing gradually and Betaproteobacteria having some OTU's increase and others decrease(6). Damann et al found Alphaproteobacteria increases from 0.8% relative abundance in the late advanced stage to 49%

relative abundance in the dry remains stage in a study focusing on remains in late decomposition from partially skeletonized, late advanced stage, to dry remains(38). Gammaproteobacteria decreases from 47% in the late advanced stage to 18% in the dry remains stage(38). Cobaugh et al 2015 found Bacteroides, the common human associated pathogen, is not present in control soils but is present in soils from the bloat stage until the end of sampling at 198 days after carcass placement(6). Emmons et al found that there were differences in community structure across bone sites that were still noticeable for up to a year(52). Verrucomicrobia was not found to be significant in either Damann et al 2015 or Emmons et al 2019 while it was prevalent through initial decomposition in Metcalf et al 2013 and Cobaugh et al 2015. As the nutrients and pH lower to levels closer to normal soil levels in dry remains, Acidobacteria begin to become prevalent again. The dramatic changes in community structure are caused by the unique environment and nutrient hotspot created during corpse decomposition. Taxa present in the dry remains stage are presented in Figure 15 and Figure 17(38).

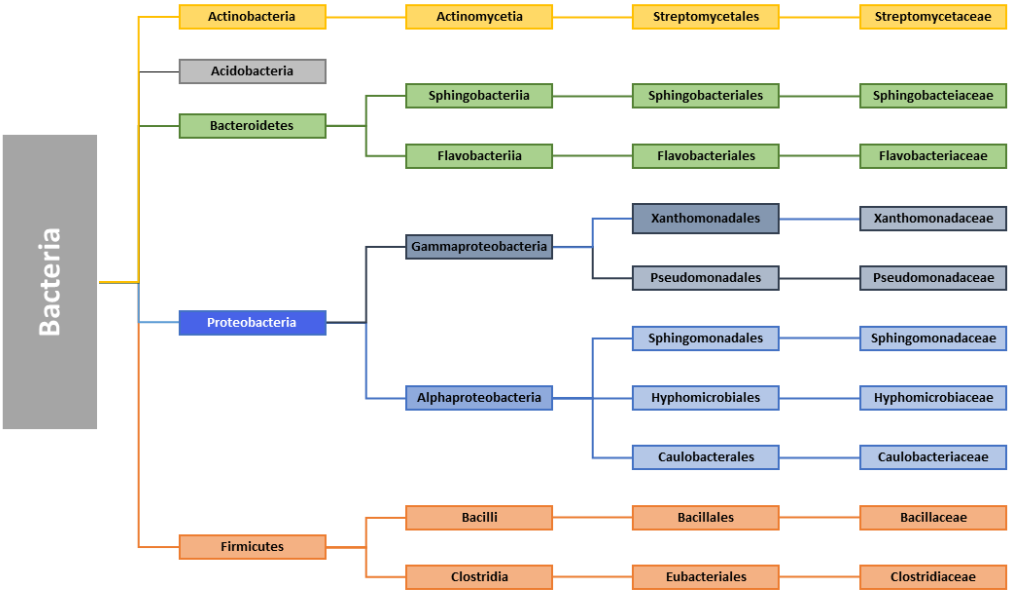

Figure 17. Postmortem Soil Microbiome Taxa Prominent During the Dry Remains Stage. Only taxa with an abundance of over 5% were included. National Center for Biotechnology Information(NCIB) database was used for all phylogenetic trees using the taxonomy browser tool(42).

In a mouse study, Metcalf et al 2016 found the initial soil community, compared to the communities of the abdominal cavity and skin, is most likely to be the source of predominant decomposer taxa(5). Across all sample sites (the skin, soil, and abdominal cavity) nearly 40% of the postmortem communities are found in the initial soil community in very low abundance(12). This is significantly higher than any other body site tested(5). Soil type, season, or host are not a significant factor for the decomposition community(5). Metcalf et al 2016 found similar soil chemistry and skin necrobiomes across three major soil types: desert, forest, and grassland(5).

Alpha diversity and richness of the soil community does not significantly change during decomposition until it increases significantly in the late advanced stage(6). This trend continues in later decomposition where Damann et al 2015 found dry remains had higher diversity than partially skeletonized remains in late advanced decay(38). This is likely caused in part by a significant increase in taxa that were previously low abundance and a general trend to the initial

community(6). Soil has significantly higher alpha diversity at every stage of decomposition than the initial postmortem gut(6). The advanced decomposition community is the most similar in structure to the initial community based on beta diversity(6). Showing the community is changing back to resident taxa.

The soil necrobiome remains largely unchanged by placement of a cadaver until after rupture(6). This initial community is dominated by Firmicutes, Actinobacteria, Acidobacteria, Betaproteobacteria and Alphaproteobacteria(6, 12). After rupture, the increase in nutrients, pH, and the gut decomposer community causes significant changes in the community(5, 6). The resident taxa of Acidobacteria, Hyphomicrobiaceae, and Prevotellaceae are no longer significant and are replaced by gut associated Gammaproteobacteria, Bacteroidetes, Firmicutes along with fly associated Xanthomonadaceae(6, 12). This change lasts until the dry remains stage when the nutrients become low again and the resident soil taxa rise in abundance(38). The skin necrobiome is in direct contact with the soil necrobiome which causes it to change in a similar manner.

4.4. Skin Necrobiome

The postmortem skin microbiome is in direct contact with the soil which causes rapid and dramatic changes throughout decomposition. The living skin microbiome is uniquely suited to thrive on the dry, nutrient deficient, and oily environment on the skin. An example of this is *Propionibacterium acnes* which is a facultative anaerobe that can thrive in the anoxic sebaceous glands(53). These taxa can utilize sweat and sebum for nutrients but are easily outcompeted when exposed to the soil environment. This causes the community to change dramatically when it is exposed to a comparatively moist, nutrient rich environment of soil. The living skin microbiome is determined by skin site due to differences present in each skin type.

Propionibacterium, Staphylococcus, and *Corynebacterium* were the most dominant genera across all skin sites(53).

In a lab experiment with mouse models, the initial postmortem microbiome is dominated by Actinobacteria, Firmicutes, Betaproteobacteria, and Gammaproteobacteria on the skin of the belly(12). The skin of the head is dominated by Epsilonproteobacteria with smaller amounts of Gammaproteobacteria and Firmicutes(12). Actinobacteria and Firmicutes are both known to be major members of the human skin microbiome(53). Firmicutes and Gammaproteobacteria begin to dominate shortly after death and Betaproteobacteria, Alphaproteobacteria, and Bacteroidetes became abundant after rupture as Gammaproteobacteria was predominant before rupture before declining to low levels(12). Alcaligenaceae and Sphingobacteriaceae were the fastest increasing OTUs on the skin and Pseudomonadaceae have one of the largest decreases in abundance(12). Xanthomonadaceae increases steadily on the skin of the belly, possibly due to proximity to gut during rupture(12). Fly associated *Ignatzschineria* and *Wohlfahrtiimonas* were abundant on the skin starting in active decay and decreased as wet biomass was consumed(44). The postmortem skin microbiome is vastly different from the soil initially but changed in a similar manner as decomposition progressed(12). This change included an increase in Sphingobacteriaceae and Xanthomonadaceae(12). Transmigration of bacteria during decomposition is a major cause of changes in the necrobiome.

4.5. Transmigration of the Necrobiome

During the initial stages of decomposition, resident microbes of the normal flora dominant in areas with high microbial abundance in life but sterile regions like the pericardial fluid and portal vein blood can remain sterile for up to 5 days(4). Using culture based techniques, 90% of pericardial fluid samples are sterile up to five days and 75% of liver samples are

sterile(4). Using 16S qPCR, the pericardial fluid samples are reduced to 60% sterile and only 10% of the liver samples are sterile at 3 days(4). Using qPCR and specific primers to a select number of species, intestinal bacteria increases in the pericardial fluid, mesenteric lymph node, and liver as PMI increases(4). Bacterial culture techniques have much higher levels of sterility than 16S qPCR showing many unculturable species are present during decomposition, reinforcing the need for more advanced techniques such as PCR and sequencing(3).

Due to discrete clustering by anatomical location on a PCoA of UniFrac distance, Pechal et al 2018 found evidence of lack of significant transmigration due to the significant diversity still present across body sites during their sampling window of less than 72 hours(3). These are presented in Figure 5(3). These were also all external sampling sites so that could have an effect on transmigration as well. As the PMI increases, so does motility pathways including motility proteins, chemotaxis, and flagellar assemblies (3). This increase is most closely correlated to the levels of Enterobacteriaceae present(3). *Proteus,* a member of Enterobacteriaceae, has been shown to increase significantly in decomposition(48). *Proteus* has a strong swarming ability making it uniquely suited to the environment by having the ability to transmigrate early in decomposition(54). *Proteus,* among others, could account for this increase in motility pathways and the swarming ability of the taxa could account for their increase in abundance. Transmigration may not be measurable on a significant level in the first 48-72 hours, but cell motility pathways do increase significantly after 48 hours, showing transmigration is starting(3).

Burcham et al 2019 found that mice which are surface sterilized in bleach after death had no significant difference on the internal postmortem microbiome(2). This conflicts with Metcalf et al 2016 who found, with their natural decomposition trials, soil is the origin of a significantly higher percentage of the gut decomposer community than originated from the gut(5). The

Burcham et al 2016 study was using laboratory conditions with no soil presence, so no soil influence was present(55). These conflicting results would need to be tested further with both natural decomposition environment and surface sterilization. Burcham et al 2016, 2019 also found that when carcasses are intranasally infected with *S. aureus*, *S. aureus* was able to infect nonsterile organs within hours, but sterile organs take up to 5 to 7 days(2, 55). They found that a single strain of *S. aureus* that is inoculated nasally postmortem can be tracked as it migrated through the body(2, 55). This strain had similar trends across organ types where it remained low initially then reached its highest point at 7 days in bone marrow and intestines or 14 days in heart and lungs before levels declined(2). The final piece of the necrobiome discussed in this paper is the transcriptome.

4.6. Transcriptome of the Necrobiome

During decomposition, the breakdown of the immune system and lysis of cells creates a nutrient rich environment for microbes. Systemic cellular death does not result in the instant death of cells throughout the body and human mRNA molecules were stable in a cadaver up to 7 days postmortem(56). Many gene transcripts had significant increases abundance after death and different abundances across postmortem times suggesting gene regulation on a cellular level even after death of the organism(18). Ferreira et al 2018 found a cascade of tissue specific transcriptional changes triggered by death which may reflect active regulation of gene expression after death(57). Using two different animal models, Hunter et al 2017 found 548 zebrafish genes and 478 mouse genes from the brain and 36 from the liver were upregulated after death(58). These upregulated genes account for only 1% of the total gene transcripts(58). Pozhitkov et al 2017 found over 1000 genes that significantly increase in abundance over the first 96 hours after death compared to living levels(18). Most genes studied peaked within 48 hours PMI(18). These

changes are unique in death and are not similar to the regulation found during hibernation(59). This differential expression of gene transcripts shows clear gene regulation at a cellular level after organismal death occurs.

Apoptosis is one of the two main routes for cellular death following organismal death. Tolbert et al 2018 found that anti-apoptotic genes are upregulated in the prostate in the first 38 hours, but by 96 and 120 hours pro-apoptotic genes dominate(60). Pro-apoptotic genes did not significantly change in expression, but the anti-apoptotic genes eventually decreased enough for apoptosis to occur(60). In another study using mice, both pro-apoptotic and anti-apoptotic gene transcripts were upregulated starting at 0.5 hours postmortem and most peaked between 12 and 48 hours(18). Apoptosis is only one the two main pathways for cellular death following organismal death, but it shows inconsistent regulation of apoptosis after cellular death.

Death significantly increases stress response genes responsible for heat shock response, hypoxia, and oxidative stress regulation(18). This is likely a last effort by individual cells and organs to attempt to maintain homeostasis. Adaptive immune response, innate immune response, and inflammation genes increase early in decomposition(18). These immune response genes peaked twice within the first 48 hours(18). Pozhitkov et al suggested this could show regulation by feedback loops(18). These studies are the beginnings of understanding not only those genes are regulated after death, but also which genes are regulated at different PMI.

5. FORENSIC USES OF THE NECROBIOME

The postmortem microbiome has potential forensic uses including identification of the postmortem interval (PMI), the manner/cause of death (M/COD), the location of a carcass, and health traits of the formally living individual. The postmortem microbiome could to help predict PMI based off the temporal presence of specific microbes, differential abundance of microbes at a specific time, machine learning algorithms, and the overall trends of community characteristics. These characteristics include gene abundance, alpha diversity, and beta diversity. Current forensic PMI practices utilize a variety of visual and physical traits as indicators for PMI including visual appearance of the carcass, forensic entomology, and temperature of the carcass. The environmental conditions of water content, insects, burial depth, and temperature can dramatically alter the timing of these changes so postmortem interval is difficult to identify. The postmortem microbiome is showing potential to be a useful addition to forensic analyses and similar to forensic entomology, the presence of certain microbial species can be indicative of postmortem interval.

5.1. PMI Using Indicator Taxa

Regardless of season, soil type, or model organism, the succession of the postmortem microbiome is predictable(5). This has led to many investigations looking for indicator taxa that can be used to assist in estimating postmortem interval. When looking at specific indicator taxa of PMI, Javan et al 2016 found that phylum level identification of specific taxon was not very predictive of PMI but genus and species were more useful(47). In a human study, Javan et al 2016found different species of the same genus were abundant at different PMI(47). This was true for species of the genus *Clostridium* and two species of the genus *Prevotella*. *Clostridium novyi* and *Prevotella bivia* were abundant at a PMI greater than 200 hours and *Prevotella timonensis*

and an unknown *Clostridium* species were abundant in early PMI at 24 hours(47). These taxa were identified as indicator taxa using random forest analysis(47).

In a study with human carcasses, Adserias et al 2016 found the phylum Tenericutes was only abundant briefly in the mouth at the onset of the bloat stage and its presence was more accurate at identifying the bloat stage than the classic visual and physical means of identification(31). They also found significant changes in the species present in the mouth in initial and early bloat stages to late bloat/active stages(31). This is presented in Figure 3(31). The prevalence of mouth associated taxa was at 75% combined abundance during the fresh stage but as decomposition progressed to the bloat stage, their abundance decreased to 25%(31). Fly associated Xanthomonadaceae became abundant in bloat. An unknown Clostridiales family becoming abundant in the bloat stage and *Bacillaceae* becoming abundant in active decay(31). Pechal et al 2018 found that Streptococcus was most abundant at early PMI (<48 hours) in the mouth and eyes(47). A study with mice models and oral sampling had conflicting results with Firmicutes increasing from the initial sampling to the 24 hour sample but they had decreased by the 6 day mark(48). They also found possible PMI identification in the class Gammaproteobacteria which increased in the mouth as PMI increased(48). More specifically, Gammaproteobacteria and the genus *Proteus* had a very strong positive linear relationships with PMI(48).

The phyla Bacteroidetes and Firmicutes which are of high abundance in the human gut were abundant still in partially skeletonized remains and Actinobacteria and Acidobacteria species that are of high abundance in the soils were more abundant in the dry remains stage(38). With intestinal sampling, Clostridiales had a positive relationship with PMI(34). While *Bacteroides* and *Lactobacillus* exponentially declined with PMI(11, 34). This is supported by

significant positive relationships between PMI and *Clostridium* and *Anaerosphaera(34)*. The same study found a significant negative relationship with PMI and *Bacteroides* and *Parabacteroides*(34). Another study using human subjects and autopsy sampling confirmed the trend in the brain, heart, liver, and spleen with Clostridiales significantly increasing with increasing PMI(30). Specifically, in the heart, they found a significant increase in relative abundance of Burkholderiales with increasing PMI(30).

A study with mouse models found significant increase in Xanthomonadaceae, Bacteroidaceae, Caulobacteraceae during active decay to advanced decay in soil(12). Xanthomonadaceae is associated with common decomposition flies but another study found Xanthomonadaceae was abundant in late decomposition with and without insect presence(39). Xanthomonadaceae may be indicative of Active and advanced decay without independent of insects(39). Enterobacteriaceae increases significantly at the end of bloat or during active decay in mouth and gut samples using animal models(12, 39, 48). This increase in Enterobacteriaceae may shows of active decay even when carcass don't rupture. A summary of necrobiome indicators of PMI are presented in Table 1**.**

PMI Range	Indicator	Location
Fresh Stage (under 24 hours)	*Prevotella timonesis*	Mouth(47)
Bloat Stage	Tenericutes	Mouth(31)
Less than 48 hours	*Streptococcus*	Mouth(31), nose, and eyes(47)
Fresh Stage	Mouth Associated Taxa	Mouth(31)
Greater than 6 days	*Proteus*	Mouth(48)
Active and Advanced Stages	Xanthomonadaceae	soil, skin, gut (12, 39, 48)
Positive relationship with PMI	Clostridiales	Intestines(34)
Positive relationship with PMI	Clostridiales	Intestines, Brain, Liver, and Spleen(30)
Negative relationship with PMI	Bacteroidales	Intestines(34)
Positive relationship with PMI	Burkholderiales	Heart(30)
Negative Relationship with PMI	Bacteroidales	Mouth(48)
Negative relationship with PMI	Beta Diversity	Skin, Soil, Mouth, rectum(39)
Negative relationship with PMI	Alpha Diversity	Skin, Ears, Eyes, Nose, Mouth, Rectum(34, 39)

Table 1. Necrobiome Indicators of PMI. PMI range indicated for and the location it applies to.

5.2. PMI Prediction with Diversity Measurements

The postmortem microbiome is initially diverse but as decomposition progresses, postmortem communities within the same study decrease in beta diversity(5, 34, 39, 44). This shows they resembled each other, with the exception of intestinal sampling(5, 34, 39, 44). This has been shown with a variety of environments and test species (5, 34, 39, 44). As decomposition progresses, communities of the mouth, skin, and rectum from humans becomes more similar to each other using an unweighted UniFrac PCoA plot(44). Another study found similar results with mice and humans where necrobiome of gravesoil and skin sites decreased in beta diversity over time(5). A PCoA using weighted UniFrac measurement from the mouth and rectum of rats were separated initially but clustered together during late PMI showing the communities changed

to become more similar(39). These studies show beta diversity decreases as decomposition progressed and the necrobiomes were becoming more similar over time(5, 39, 44).

Like beta diversity, richness of the postmortem microbiome decreases for certain anatomical locations as decomposition progresses. Alpha diversity significantly decreases in human eye, nose, ear, and mouth samples for samples greater than 48 hours but not the rectal sample site(3). Alpha diversity was significantly higher in the necrobiome of the uterus and prostate than the heart, brain, and liver(30). In mice models, the alpha diversity of oral samples decreases over time but the difference from the initial alpha diversity measurement was not significant until the sample at 6 days(48). The alpha diversity of the gut postmortem microbiome increased as decomposition increased while beta diversity decreased(34). This conflicts with the trend from the external sampling sites but this difference could be attributed to sampling in this study at a significantly later PMI(34).

5.3. Machine Learning Analysis of PMI

Metcalf et al 2013 presented the changes of the postmortem microbiome using mouse models as a microbial clock and could accurately predict the PMI (12). Metcalf et al was able to use the postmortem microbiome of the skin on the head of mice to estimate PMI with an accuracy of 3.30+/- 2.52 days(12). This is presented in Figure 6(12). They prove skin and soil sites were more accurate in predicting PMI than gut samples(12). Using Random Forest models across a variety of test organisms and sampling sites, 16S rRNA with bacterial and archaeal phylum level data gravesoil data had the lowest error(29). A Random Forest model created with necrobiome data could predict PMI within 2-3 days though the first two weeks of decomposition(5). This Random Forest model was accurate across soil types(5). This was tested by using the necrobiome associated with one soil type was used to train the model and predict

the PMI with the bacterial community of another soil type(5). Using a different machine learning approach, Johnson et al found that k-Nearest Neighbor regression was the most accurate machine learning approach for predicting PMI with their combined ear and nasal microbiomes(41). This approach could predict the PMI of a body within 55 accumulated degree days (ADD)(41). This corresponds to 2 days at an average temperature of 27.5°C.

Belk et al 2018 found that Random Forest regression analysis with gravesoil and skin 16S rRNA was most accurate for PMI predictions at the phyla level(29). There are conflicting results depending on the model organism and machine learning algorithm(29, 61). Javan et al 2017 used specific taxa presence and abundance found in human autopsy sampling to predict PMI and found the genus was more accurate(61). Belk et al 2018 used Random Forest regression of multiple data sets including human and mice, and a variety of sampling sites to predict PMI(29). These are very different types of analyses and shows the variety of results that can be found from different forms of microbiome analyses.

5.4. Transcriptome Analysis to Estimate PMI

Besides species present, changes in nucleic acid and gene transcript abundances are showing potential use to predict PMI as well. There is a consistent, significant decline in ribonuclease genes(57). This study hypothesized a possible unique PMI prediction technique involving RNA degradation levels but only had moderate success due to small sample size(57). Groups of gene transcripts that are upregulated after death can be used to predict PMI(58). A group of 7 mouse liver genes and 7 mouse brain genes could accurately predict PMI with R^2 values of 0.97 and 0.95 respectively(58). Only genes that were upregulated after death were used in these equations because only 1% of the transcriptome is upregulated after death and they are likely directly related organismal death(58).

5.5. Prediction of Manner and Cause of Death

Another potential use for postmortem microbiome data is the identification of living characteristics and manner/causes of death (M/COD). There is a significant positive relationship between the alpha diversity of the postmortem microbiome and probability of violent deaths(3). There is a 65.2% increase chance of violent death for every unit of α-diversity increase(3). They also found a negative relationship between bacterial postmortem alpha diversity and probability of death by heart disease with a 28% decreased chance of heart disease COD for every unit of diversity increase(3). Samples less than 24 hours PMI were used because they performed better as indicators of M/COD(3). People who died from heart disease have the highest beta diversity and used this to successfully predict the cause of death between heart disease or drug related cases 79% of the time(40). This study was able to identify suicides with a 58.1% success rate and were able to determine if COD of gunshot wound was by homicide or suicide accurately 93.1% of the time (40). The beta diversity is highest in cases of natural death(40). There was a significant increase in beta diversity in cases of cardiovascular death compared to gunshot wounds, blunt force trauma, and drug CODs(40). Homicides had lowest beta diversity(40). In a recent study with humans, Enterobacteriaceae, Chitinophagaceae, and $MLE_{1\text{-}12}$ had a strong positive association (>20 $\log_2$ fold change relative to other CODs)(30). Natural deaths and deaths by homicide were slightly negatively associated (5 $\log_2$ change relative to other CODs) with Streptococcaceae and Lactobacillaceae(30). Suicide has a strong negative association with Peptostreptococcaceae(>20 $\log_2$ fold change relative to other CODs)(30).

5.6. Location Identification

The postmortem microbiome has potential to aid the field of forensics in estimation of PMI and manner of death but there is early evidence of potential to identify the geographical

location of a carcass and even the anatomical location of an unknown organ. There is a significantly higher number of pathogens in postmortem microbiomes of people who live in neighborhoods with high levels of blight compared to areas with high levels of green remediation(62). Neighborhood blight is a measure of the number of abandoned buildings or vacant lots in an area and green remediation was used as a measure of available greenspace(62). Microbial alpha and beta diversity were positively associated with neighborhood green remediation and negatively associated with blight(62). Green remediation had the highest positive effect in the richness of male rectum communities and the beta diversity of female noses(62). Blight had the largest negative effect on richness and beta diversity of the nose and mouth of men. This is initial evidence that the postmortem microbiome can be used by forensic investigators to identify the type of environment the deceased person lived in. There are some conflicting results, but it has potential uses, nonetheless.

During forensic investigation, unknown tissue fragments may be found at crime scenes the and the postmortem microbiome has potential to aid in indemnifying these unknown tissues. Organ type was the strongest grouping factor for UniFrac distance measures of the necrobiome(3, 30). Liver tissue is able to be successfully identified as being from the liver based off tissue specific gene biomarkers(56). This was just a proof-of-concept experiment that shows some possible future impacts the postmortem microbiome can have on forensics.

6. CONCLUSIONS

The most common ways the postmortem microbiome is analyzed is with relative abundance, alpha diversity, beta diversity, and machine learning algorithms. Relative abundance is a method used to compare the abundance of each taxon in a sample to the total number of reads present in the sample. Alpha diversity is a measure of diversity within a sample using richness, evenness, or a combination of the two. Richness is the total number of different taxon present in a population and evenness is the measure of distribution of abundances in a population. The combination of these two like in a Simpson's Index, can give a new measure of alpha diversity in a community if separate richness and evenness calculations are not desired. Beta diversity is the diversity between samples and is used to measure how similar or dissimilar samples are to each other. This is calculated through distance metrics like Bray-Curtis dissimilarity and UniFrac distances and are commonly visualized on a Principal Coordinate Analysis Plot (PCoA). Machine learning models such as Random Forest regression or k-Nearest Neighbor regression are algorithms that are used in microbiome studies to classify groups of genome data into groups. Machine learning is commonly used with the postmortem microbiome to estimate PMI.

The initial postmortem microbiome of a carcass is dominated by resident taxa which are able to flourish after death as the cells lyse and the immune systems breaks down. Anaerobes like Clostridiaceae, Enterobacteriales, along with fly associated Xanthomonadaceae become dominant after rupture. The soil underneath a decaying carcass is not significantly changed by carcass placement until purge and rupture when a large influx of nutrients and the gut necrobiome change the community significantly. The soil necrobiome is dominated by gut and fly associated taxa until dry remains when the soil taxa become abundant again. The postmortem

skin microbiome is initially dominated by resident taxa, but it quickly changes to be similar to the soil community after it is placed on soil.

PMI is essential to forensic investigations; however, current methods only give a rough range of time and are greatly affected by the environment. The postmortem microbial communities changed in a clock-like manner that provided an estimate of absolute PMI is similar to using the development of fly larvae to estimate PMI(5). However, entomological PMI identification methods are limited by corpse accessibility to insects and variable insect presence by season, resulting in PMI estimates in the range of weeks, months, and years(63). Postmortem microbiome has the potential to be a new tool to increase the accuracy of PMI determination when other ways are inaccurate unable to be utilized.

The postmortem microbiome is a growing field of study that many potential impacts, both in forensics and other. It follows a predictable succession of changes, and the catalogue of these changes continue to expand. Community factors such as relative abundance of taxa, alpha diversity, beta diversity, gene transcripts can all be used to track these changes. Further understanding of these changes have the potential be used forensically to aid in PMI determination, manner/cause of death identification, and the living location of deceased persons. The postmortem microbiome field is limited by the availability of ethically sourced corpses of human and animal models, but as more data becomes available, more accurate predictions and valuable insights will become available.

REFERENCES

1. Benbow ME, Lewis AJ, Tomberlin JK, Pechal JL. 2013. Seasonal Necrophagous Insect Community Assembly During Vertebrate Carrion Decomposition. Journal of Medical Entomology 50:440-450.

2. Burcham ZM, Pechal JL, Schmidt CJ, Bose JL, Rosch JW, Benbow ME, Jordan HR. 2019. Bacterial Community Succession, Transmigration, and Differential Gene Transcription in a Controlled Vertebrate Decomposition Model. Frontiers in Microbiology 10:745.

3. Pechal JL, Schmidt CJ, Jordan HR, Benbow ME. 2018. A large-scale survey of the postmortem human microbiome, and its potential to provide insight into the living health condition. Scientific Reports 8:5724.

4. Tuomisto S, Karhunen PJ, Vuento R, Aittoniemi J, Pessi T. 2013. Evaluation of Postmortem Bacterial Migration Using Culturing and Real-Time Quantitative PCR. Journal of Forensic Sciences 58:910-916.

5. Metcalf JL, Xu ZZ, Weiss S, Lax S, Van Treuren W, Hyde ER, Song SJ, Amir A, Larsen P, Sangwan N, Haarmann D, Humphrey GC, Ackermann G, Thompson LR, Lauber C, Bibat A, Nicholas C, Gebert MJ, Petrosino JF, Reed SC, Gilbert JA, Lynne AM, Bucheli SR, Carter DO, Knight R. 2016. Microbial community assembly and metabolic function during mammalian corpse decomposition. Science 351:158.

6. Cobaugh KL, Schaeffer SM, DeBruyn JM. 2015. Functional and Structural Succession of Soil Microbial Communities below Decomposing Human Cadavers. PLOS ONE 10:e0130201.

7. Payne JA. 1965. A Summer Carrion Study of the Baby Pig Sus Scrofa Linnaeus. Ecology 46:592-602.

8. Carter DO, Yellowlees D, Tibbett M. 2007. Cadaver decomposition in terrestrial ecosystems. Naturwissenschaften 94:12-24.

9. Clark MA, Worrell MB, Pless JE. 1997. Postmortem changes in soft tissues. Forensic taphonomy: the postmortem fate of human remains:151-164.

10. Janaway RC, Percival S, Wilson A. 2009. Decomposition of Human Remains, p 313-334.

11. Hauther KA, Cobaugh KL, Jantz LM, Sparer TE, DeBruyn JM. 2015. Estimating Time Since Death from Postmortem Human Gut Microbial Communities. Journal of Forensic Sciences 60:1234-1240.

12. Metcalf JL, Wegener Parfrey L, Gonzalez A, Lauber CL, Knights D, Ackermann G, Humphrey GC, Gebert MJ, Van Treuren W, Berg-Lyons D, Keepers K, Guo Y, Bullard J, Fierer N, Carter DO, Knight R. 2013. A microbial clock provides an accurate estimate of the postmortem interval in a mouse model system. eLife 2:e01104-e01104.

13. Tóth E, Kovács G, Schumann P, Kovács AL, Steiner U, Halbritter A, Márialigeti K. 2001. Schineria larvae gen. nov., sp. nov., isolated from the 1st and 2nd larval stages of Wohlfahrtia magnifica (Diptera: Sarcophagidae). International Journal of Systematic and Evolutionary Microbiology 51:401-407.

14. Lawen A. 2003. Apoptosis—an introduction. BioEssays 25:888-896.

15. Galluzzi L, Vitale I, Aaronson SA, Abrams JM, Adam D, Agostinis P, Alnemri ES, Altucci L, Amelio I, Andrews DW, Annicchiarico-Petruzzelli M, Antonov AV, Arama E, Baehrecke EH, Barlev NA, Bazan NG, Bernassola F, Bertrand MJM, Bianchi K, Blagosklonny MV, Blomgren K, Borner C, Boya P, Brenner C, Campanella M, Candi E, Carmona-Gutierrez D, Cecconi F, Chan FKM, Chandel NS, Cheng EH, Chipuk JE, Cidlowski JA, Ciechanover A, Cohen GM, Conrad M, Cubillos-Ruiz JR, Czabotar PE, D'Angiolella V, Dawson TM, Dawson VL, De Laurenzi V, De Maria R, Debatin K-M, DeBerardinis RJ, Deshmukh M, Di Daniele N, Di Virgilio F, Dixit VM, Dixon SJ, et al. 2018. Molecular mechanisms of cell death: recommendations of the Nomenclature Committee on Cell Death 2018. Cell Death & Differentiation 25:486-541.

16. Galluzzi L, Maiuri MC, Vitale I, Zischka H, Castedo M, Zitvogel L, Kroemer G. 2007. Cell death modalities: classification and pathophysiological implications. Cell Death & Differentiation 14:1237-1243.

17. Chowdhury I, Tharakan B, Bhat GK. 2008. Caspases — An update. Comparative Biochemistry and Physiology Part B: Biochemistry and Molecular Biology 151:10-27.

18. Pozhitkov AE, Neme R, Domazet-Lošo T, Leroux BG, Soni S, Tautz D, Noble PA. 2017. Tracing the dynamics of gene transcripts after organismal death. Open Biology 7:160267.

19. Schloss PD, Handelsman J. 2005. Introducing DOTUR, a computer program for defining operational taxonomic units and estimating species richness. Applied and environmental microbiology 71:1501-1506.

20. Hoogenboom J, van der Gaag KJ, de Leeuw RH, Sijen T, de Knijff P, Laros JFJ. 2017. FDSTools: A software package for analysis of massively parallel sequencing data with the ability to recognise and correct STR stutter and other PCR or sequencing noise. Forensic Science International: Genetics 27:27-40.

21. Glenn TC. 2011. Field guide to next-generation DNA sequencers. Molecular Ecology Resources 11:759-769.

22. DeSantis TZ, Hugenholtz P, Larsen N, Rojas M, Brodie EL, Keller K, Huber T, Dalevi D, Hu P, Andersen GL. 2006. Greengenes, a chimera-checked 16S rRNA gene database and workbench compatible with ARB. Applied and environmental microbiology 72:5069-5072.

23. McDonald D, Price MN, Goodrich J, Nawrocki EP, DeSantis TZ, Probst A, Andersen GL, Knight R, Hugenholtz P. 2012. An improved Greengenes taxonomy with explicit ranks for ecological and evolutionary analyses of bacteria and archaea. ISME J 6:610-8.

24. Cole JR, Chai B, Farris RJ, Wang Q, Kulam-Syed-Mohideen AS, McGarrell DM, Bandela AM, Cardenas E, Garrity GM, Tiedje JM. 2007. The ribosomal database project (RDP-II): introducing myRDP space and quality controlled public data. Nucleic Acids Research 35:D169-D172.

25. Quast C, Pruesse E, Yilmaz P, Gerken J, Schweer T, Yarza P, Peplies J, Glöckner FO. 2013. The SILVA ribosomal RNA gene database project: improved data processing and web-based tools. Nucleic Acids Res 41:D590-6.

26. Johnson M, Zaretskaya I, Raytselis Y, Merezhuk Y, McGinnis S, Madden TL. 2008. NCBI BLAST: a better web interface. Nucleic Acids Research 36:W5-W9.

27. Amir A, McDonald D, Navas-Molina JA, Kopylova E, Morton JT, Zech Xu Z, Kightley EP, Thompson LR, Hyde ER, Gonzalez A, Knight R. 2017. Deblur Rapidly Resolves Single-Nucleotide Community Sequence Patterns. mSystems 2:e00191-16.

28. Lee CK, Herbold CW, Polson SW, Wommack KE, Williamson SJ, McDonald IR, Cary SC. 2012. Groundtruthing next-gen sequencing for microbial ecology-biases and errors in community structure estimates from PCR amplicon pyrosequencing. PloS one 7:e44224-e44224.

29. Belk A, Xu ZZ, Carter DO, Lynne A, Bucheli S, Knight R, Metcalf JL. 2018. Microbiome Data Accurately Predicts the Postmortem Interval Using Random Forest Regression Models. Genes 9:104.

30. Lutz H, Vangelatos A, Gottel N, Osculati A, Visona S, Finley SJ, Gilbert JA, Javan GT. 2020. Effects of Extended Postmortem Interval on Microbial Communities in Organs of the Human Cadaver. Frontiers in Microbiology 11:3127.

31. Adserias-Garriga J, Quijada NM, Hernandez M, Rodríguez Lázaro D, Steadman D, Garcia-Gil LJ. 2017. Dynamics of the oral microbiota as a tool to estimate time since death. Molecular Oral Microbiology 32:511-516.

32. Willis AD. 2019. Rarefaction, Alpha Diversity, and Statistics. Frontiers in Microbiology 10.

33. Chao A, Chiu C-H, Jost L. 2016. Phylogenetic Diversity Measures and Their Decomposition: A Framework Based on Hill Numbers, p 141-172. *In* Pellens R, Grandcolas P (ed), Biodiversity Conservation and Phylogenetic Systematics: Preserving our evolutionary heritage in an extinction crisis. Springer International Publishing, Cham.

34. DeBruyn JM, Hauther KA. 2017. Postmortem succession of gut microbial communities in deceased human subjects. PeerJ 5:e3437.

35. Clarke KR, Somerfield PJ, Chapman MG. 2006. On resemblance measures for ecological studies, including taxonomic dissimilarities and a zero-adjusted Bray–Curtis coefficient for denuded assemblages. Journal of Experimental Marine Biology and Ecology 330:55-80.

36. Lozupone C, Lladser ME, Knights D, Stombaugh J, Knight R. 2011. UniFrac: an effective distance metric for microbial community comparison. The ISME Journal 5:169-172.

37. Lozupone CA, Hamady M, Kelley ST, Knight R. 2007. Quantitative and Qualitative β Diversity Measures Lead to Different Insights into Factors That Structure Microbial Communities. Applied and Environmental Microbiology 73:1576.

38. Damann FE, Williams DE, Layton AC. 2015. Potential Use of Bacterial Community Succession in Decaying Human Bone for Estimating Postmortem Interval. Journal of Forensic Sciences 60:844-850.

39. Guo J, Fu X, Liao H, Hu Z, Long L, Yan W, Ding Y, Zha L, Guo Y, Yan J, Chang Y, Cai J. 2016. Potential use of bacterial community succession for estimating post-mortem interval as revealed by high-throughput sequencing. Scientific Reports 6:24197.

40. Kaszubinski SF, Pechal JL, Smiles K, Schmidt CJ, Jordan HR, Meek MH, Benbow ME. 2020. Dysbiosis in the Dead: Human Postmortem Microbiome Beta-Dispersion as an Indicator of Manner and Cause of Death. Frontiers in Microbiology 11:2212.

41. Johnson HR, Trinidad DD, Guzman S, Khan Z, Parziale JV, DeBruyn JM, Lents NH. 2016. A Machine Learning Approach for Using the Postmortem Skin Microbiome to Estimate the Postmortem Interval. PLOS ONE 11:e0167370.

42. Information NCfB. 2021. Taxonomy Browser. https://www.ncbi.nlm.nih.gov/Taxonomy/CommonTree/wwwcmt.cgi. Accessed 04/22/2021.

43. Tóth EM, Hell É, Kovács G, Borsodi AK, Márialigeti K. 2006. Bacteria Isolated from the Different Developmental Stages and Larval Organs of the Obligate Parasitic Fly, Wohlfahrtia magnifica (Diptera: Sarcophagidae). Microbial Ecology 51:13-21.

44. Hyde ER, Haarmann DP, Petrosino JF, Lynne AM, Bucheli SR. 2015. Initial insights into bacterial succession during human decomposition. International Journal of Legal Medicine 129:661-671.

45. Marsh PD. 2000. Role of the Oral Microflora in Health. Microbial Ecology in Health and Disease 12:130-137.

46. Deo PN, Deshmukh R. 2019. Oral microbiome: Unveiling the fundamentals. Journal of oral and maxillofacial pathology : JOMFP 23:122-128.

47. Javan GT, Finley SJ, Can I, Wilkinson JE, Hanson JD, Tarone AM. 2016. Human Thanatomicrobiome Succession and Time Since Death. Scientific Reports 6:29598.

48. Dong K, Xin Y, Cao F, Huang Z, Sun J, Peng M, Liu W, Shi P. 2019. Succession of oral microbiota community as a tool to estimate postmortem interval. Scientific Reports 9:13063.

49. Hewelke E, Górska EB, Gozdowski D, Korc M, Olejniczak I, Prędecka A. 2020. Soil Functional Responses to Natural Ecosystem Restoration of a Pine Forest Peucedano-Pinetum after a Fire. Forests 11.

50. Lauber CL, Hamady M, Knight R, Fierer N. 2009. Pyrosequencing-based assessment of soil pH as a predictor of soil bacterial community structure at the continental scale. Applied and environmental microbiology 75:5111-5120.

51. Ward NL, Challacombe JF, Janssen PH, Henrissat B, Coutinho PM, Wu M, Xie G, Haft DH, Sait M, Badger J, Barabote RD, Bradley B, Brettin TS, Brinkac LM, Bruce D, Creasy T, Daugherty SC, Davidsen TM, DeBoy RT, Detter JC, Dodson RJ, Durkin AS, Ganapathy A, Gwinn-Giglio M, Han CS, Khouri H, Kiss H, Kothari SP, Madupu R, Nelson KE, Nelson WC, Paulsen I, Penn K, Ren Q, Rosovitz MJ, Selengut JD, Shrivastava S, Sullivan SA, Tapia R, Thompson LS, Watkins KL, Yang Q, Yu C, Zafar N, Zhou L, Kuske CR. 2009. Three genomes from the phylum Acidobacteria provide insight into the lifestyles of these microorganisms in soils. Applied and environmental microbiology 75:2046-2056.

52. Emmons AL, Mundorff AZ, Keenan SW, Davoren J, Andronowski JM, Carter DO, Debruyn JM. 2019. Patterns of microbial colonization of human bone from surface-decomposed remains. Cold Spring Harbor Laboratory Press, Cold Spring Harbor.

53. Byrd AL, Belkaid Y, Segre JA. 2018. The human skin microbiome. Nature reviews Microbiology 16:143-155.

54. Stuart CA, Wheeler KM, McGann V, Howard I. 1946. Motility and Swarming of Some Enterobacteriaceae. Journal of bacteriology 52:519-525.

55. Burcham ZM, Hood JA, Pechal JL, Krausz KL, Bose JL, Schmidt CJ, Benbow ME, Jordan HR. 2016. Fluorescently labeled bacteria provide insight on post-mortem microbial transmigration. Forensic Science International 264:63-69.

56. Javan GT, Hanson E, Finley SJ, Visonà SD, Osculati A, Ballantyne J. 2020. Identification of cadaveric liver tissues using thanatotranscriptome biomarkers. Scientific Reports 10:6639.

57. Ferreira PG, Muñoz-Aguirre M, Reverter F, Sá Godinho CP, Sousa A, Amadoz A, Sodaei R, Hidalgo MR, Pervouchine D, Carbonell-Caballero J, Nurtdinov R, Breschi A, Amador R, Oliveira P, Çubuk C, Curado J, Aguet F, Oliveira C, Dopazo J, Sammeth M, Ardlie KG, Guigó R. 2018. The effects of death and post-mortem cold ischemia on human tissue transcriptomes. Nature Communications 9:490.

58. Hunter MC, Pozhitkov AE, Noble PA. 2017. Accurate predictions of postmortem interval using linear regression analyses of gene meter expression data. Forensic science international 275:90-101.

59. Hadj-Moussa H, Watts AJ, Storey KB. 2019. Genes of the undead: hibernation and death display different gene profiles. FEBS Letters 593:527-532.

60. Tolbert M, Finley SJ, Visonà SD, Soni S, Osculati A, Javan GT. 2018. The thanatotranscriptome: Gene expression of male reproductive organs after death. Gene 675:191-196.

61. Javan GT, Finley SJ, Smith T, Miller J, Wilkinson JE. 2017. Cadaver Thanatomicrobiome Signatures: The Ubiquitous Nature of Clostridium Species in Human Decomposition. Frontiers in Microbiology 8:2096.

62. Pearson AL, Rzotkiewicz A, Pechal JL, Schmidt CJ, Jordan HR, Zwickle A, Benbow ME. 2019. Initial Evidence of the Relationships between the Human Postmortem Microbiome and Neighborhood Blight and Greening Efforts. Annals of the American Association of Geographers 109:958-978.

63. Amendt J, Campobasso Cp Fau - Gaudry E, Gaudry E Fau - Reiter C, Reiter C Fau - LeBlanc HN, LeBlanc Hn Fau - Hall MJR, Hall MJ. 2007. Best practice in forensic entomology--standards and guidelines. International Journal of Medicine 121:90-104.